Electronic Supplementary Material (ESI) for Dalton Transactions.
This journal is © The Royal Society of Chemistry 2023

Supporting Information
for

Fluorescent Phenothiazine-Boranil Complexes for Hypochlorite Sensing

Hong Wang,[aΔ] Changli Zhang,[bΔ] Zhiyong Jiang,[c] Li Xu,*[a] and Zhipeng Liu*[c,d]

[a] College of Science, Nanjing Forestry University, Nanjing 210037, China. Email: xuliqby@njfu.edu.cn.

[b] School of Environmental Science, Nanjing Xiaozhuang University, Nanjing 211171, China.

[c] College of Materials Science and Engineering, Nanjing Forestry University, Nanjing 210037, China. Email: zpliu@njfu.edu.cn.

[d] Co-Innovation Center of Efficient Processing and Utilization of Forest Resources, Nanjing Forestry University, Nanjing 210037, China.

[Δ] These authors contribute equally to this work.

Table of Contents

1. Methods and materials

Solvents were dried before use by conventional methods in organometallic chemistry. Commercially available chemicals were used as received. By using the Schlenk technique, all air sensitive compounds reacted under the protection of the inert gases. Flash column chromatography (100-200 mesh) was performed using silica gel purchased from Ding Kang Silica Gel Co. The ^{1}H and ^{13}C NMR spectra were recorded on a Bruker AV-600/-400 spectrometer at 600 MHz and 400 MHz for ^{1}H NMR, and 150 MHz for ^{13}C NMR. Chemical shifts in ppm compared to $Si(CH_3)_4$ (^{1}H) are reported. ^{1}H NMR coupling constants (*J*) are reported in Hertz (Hz), and multiplicities are expressed as follows: s (singlet), d (doublet), t (triplet), m (multiplet). High-resolution mass spectra (HRMS) were recorded on an LCQ (ESI-MS, thermo Finnigan) mass spectrometer. Confocal laser scanning microscopy (CLSM) images were performed on a Zeiss lSM710 confocal laser scanning microscope.

2. Synthesis

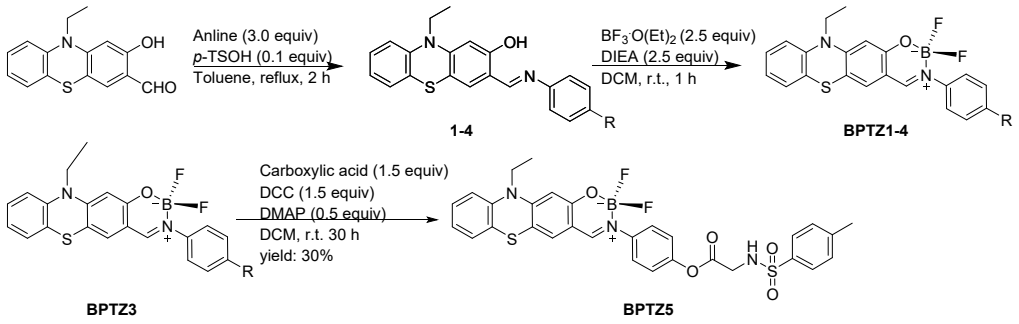

Scheme S1. Synthesis of Probes.

Synthesis of compounds 1-4

10-ethyl-2-hydroxy-3-carbaldehyde-10*H*-phenothiazine was prepared following a previous report[1]. To a solution of aniline (3 equiv) and *p*-TsOH (0.1 equiv) in dry toluene was added 10-ethyl-2-hydroxy-3-carbaldehyde-10*H*-phenothiazine (1 equiv). The resulting solution was refluxed for 1 h. After cooling down to room temperature, the resulting precipitate was filtered, recrystallized from ethanol, washed with n-hexane and dried under vacuum, to give the target product.

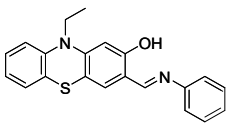

Compound **1**: A dark red solid was obtained in 81% yield. **^{1}H NMR** (600 MHz, $CDCl_3$) δ/ppm =13.71(s, 1H), 8.43 (s, 1H), 7.40 (t, J = 7.8Hz, 2H), 7.24 (s, 1H), 7.19(t, J = 7.8Hz, 2H), 7.12(d, J = 7.2 Hz, 1H) 7.05 (s, 1H), 6.95–6.91 (m, 2H), 6.69 (d, J = 8.4 Hz, 1H), 6.51 (s, 1H), 3.98–3.95 (m, 2H), 1.46 (t, J = 6.6 Hz, 3H). **^{13}C NMR** (150 MHz, $CDCl_3$) δ/ppm =158.6, 141.6, 129.6, 128.2, 127.7, 127.4, 127.3, 126.7, 124.5, 124.0, 123.1, 120.9, 116.5, 116.1, 115.72, 42.6, 12.7. **HRMS** (ESI^+): calcd. for $C_{21}H_{18}N_2OS$: $[M-H]^-$ = 345.1056, found: $[M-H]^-$ = 345.1072.

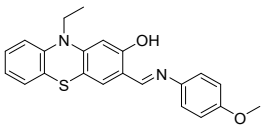

Compound **2**: A yellow solid was obtained in 76% yield. **^{1}H NMR** (400 MHz, $CDCl_3$) δ/ppm =13.81 (s, 1H), 8.40 (s, 1H), 7.23 (d, J = 8.0 Hz, 2H), 7.17–7.10 (m, 2H), 7.02 (s, 1H), 6.93–6.89 (m, 4H), 6.50 (s, 1H), 3.97–3.92 (m, 2H), 3.83 (s, 3H), 1.45 (t, J = 6.8 Hz, 3H). **^{13}C NMR** (150 MHz, $CDCl_3$) δ/ppm = 162.8, 158.5, 158.4, 149.2, 143.3, 141.1, 129.4, 127.3, 124.0, 123.0, 122.1, 115.6, 114.7, 114.4, 112.7, 103.7, 55.6, 42.5, 12.9. **HRMS** (ESI^+): calcd. for $C_{22}H_{20}N_2O_2S$: $[M]^-$ = 376.1245, found: $[M]^-$= 376.1208.

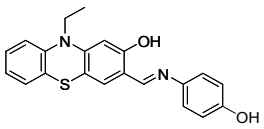

Compound **3**: A red solid was obtained in 95% yield. **^{1}H NMR** (400 MHz, DMSO) δ/ppm =13.83 (s, 1H), 9.60 (s, 1H), 8.73 (s, 1H), 7.29 (s, 1H), 7.24 (d, J = 7.6 Hz, 2H), 7.20 (d, J = 7.6 Hz, 1H), 7.15 (d, J = 7.6 Hz, 1H), 7.06 (d, J = 8.0 Hz, 1H), 6.97 (t, J = 7.2 Hz, 1H), 6.81 (d, J = 8.0 Hz, 2H), 6.53 (s, 1H), 3.98–3.93 (m, 2H), 1.32 (t, J = 6.4 Hz, 3H). **^{13}C NMR** (150 MHz, $CDCl_3$) δ/ppm = 161.8, 158.5, 156.5, 148.3, 142.7, 139.0, 129.4, 127.6, 127.0, 122.9, 122.8, 122.2, 115.9, 114.3, 111.3, 103.3, 41.6, 12.5. **HRMS** (ESI^+): calcd. for $C_{21}H_{18}N_2O_2S$: $[M-H]^-$ =361.1005, found: $[M-H]^-$ =361.1021.

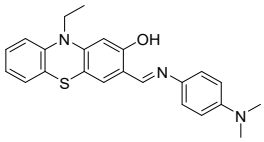

Compound **4:** A dark yellow solid was obtained in 97% yield. **^{1}H NMR** (400 MHz, $CDCl_3$) δ/ppm = 14.17 (s, 1H), 8.41 (s, 1H), 7.23 (d, J = 8.8 Hz, 2H), 7.17–7.11 (m, 2H), 7.01 (s, 1H), 6.94–6.90 (m, 2H), 6.74 (d, J = 8.8 Hz, 2H), 6.49 (s, 1H), 3.98–3.93 (m, 2H), 2.99 (s, 6H), 1.46 (t, J = 6.8 Hz, 3H). **^{13}C NMR** (150 MHz, $CDCl_3$) δ/ppm = 163.0, 155.9, 149.7, 148.8, 143.5, 136.7, 129.1, 127.3, 124.1, 122.8, 121.9, 115.5, 114.7, 113.0, 112.5, 103.8, 42.4, 40.7, 13.0. **HRMS** (ESI^+): calcd. for $C_{23}H_{23}N_3OS$: $[M]^-$ = 389.1562, found: $[M]^-$ = 389.1527.

Synthesis of BPTZ1-4

To a stirred solution of compounds **1-4** (1equiv) in dry dichloroethane (DCM) at room temperature was added BF_3•OEt_2 (2.5 equiv).[2] A color change occurs reveals the formation of an intermediary. After 15 minutes, *N,N*-diisopropylethylamine (2.5 equiv) is added to form the desired boranil. After cooling down to room temperature, the resulting mixture was washed with a saturated solution of $NaHCO_3$, then extracted with DCM and washed with brine. Organic layers were dried over $MgSO_4$ and evaporated under vacuum. The product was purified by silica gel chromatography.

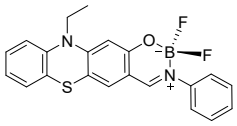

BPTZ1 : A dark red solid was obtained in 70% yield (DCM). **^{1}H NMR** (600 MHz, $CDCl_3$) δ/ppm = 8.11 (s, 1H), 7.53 (d, J = 7.8 Hz, 2H), 7.48–7.39 (m, 2H), 7.42 (t, J = 7.8 Hz, 1H), 7.20–7.17 (m, 1H), 7.10 (dd, J = 7.2, 1.2 Hz, 1H), 7.02 (s, 1H), 7.00–6.97 (m, 2H), 6.49 (s, 1H), 3.99–3.96 (m, 2H), 1.47 (t, J = 7.2 Hz, 3H). **^{13}C NMR** (150 MHz, $CDCl_3$) δ/ppm = 161.3, 159.7, 154.5, 142.8, 141.5, 129.7, 128.7, 128.4, 127.8, 127.3, 124.0, 123.5, 123.0, 116.4, 115.1, 111.1, 103.6, 43.3, 12.7. **HRMS** (ESI^+): calcd. for $C_{21}H_{17}BF_2N_2OS$: $[M + Na]^+$ = 437.1015, found: $[M + Na]^+$ = 437.1012.

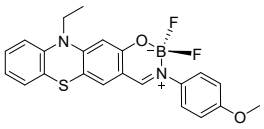

BPTZ2 : A red solid was obtained in 57% yield (petroleum ether (P): DCM =1: 5, *v*/*v*). **^{1}H NMR** (600 MHz, $CDCl_3$) δ/ppm = 8.07 (s, 1H), 7.45 (d, J = 9.0 Hz, 2H), 7.20–7.17 (m, 1H), 7.09 (dd, J = 7.2, 1.2 Hz, 1H), 7.02 (s, 1H), 7.00–6.98 (m, 1H), 6.97–6.95 (m, 3H), 6.50 (s, 1H), 3.99–3.96 (m, 2H), 3.84 (s, 3H), 1.47 (t, J = 7.2 Hz, 3H). **^{13}C NMR** (150 MHz, $CDCl_3$) δ/ppm = 161.1, 159.9, 158.7, 154.2, 141.6, 135.9, 128.2, 127.8, 127.3, 124.6, 124.0, 123.0, 116.3, 115.0, 114.8, 111.2, 103.7, 55.7, 43.3, 12.8. **HRMS** (ESI^+): calcd. for $C_{22}H_{19}BF_2N_2O_2S$: $[M + Na]^+$ = 447.1120, found: $[M + Na]^+$ = 440.1142.

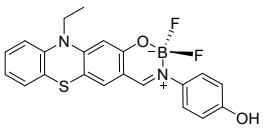

BPTZ3: A red solid was obtained in 54% yield (ethyl acetate (EA): DCM =1: 10, *v*/*v*). **^{1}H NMR** (600 MHz, DMSO) δ/ppm = 8.07 (s, 1H), 7.39 (d, J = 9.0 Hz, 2H), 7.19–7.16 (m, 1H), 7.09 (dd, J = 7.8, 1.8 Hz, 1H), 7.05 (s, 1H), 7.00–6.96 (m, 2H), 6.90–6.89 (m, 2H), 6.53 (s, 1H), 5.05 (s, 1H), 4.00–3.97 (m, 2H), 1.48 (t, J = 7.2 Hz, 3H). **^{13}C NMR** (150 MHz, $CDCl_3$) δ/ppm = 160.7, 159.7, 157.6, 153.0, 141.2, 134.0, 129.4, 127.9, 127.0, 124.4, 123.8, 121.8, 116.5, 115.8, 113.1, 111.1, 103.1, 42.3, 12.3. **HRMS** (ESI^+): calcd. for $C_{21}H_{17}BF_2N_2O_2S$: $[M-H]^-$ =409.0988, found: $[M-H]^-$

=409.0992.

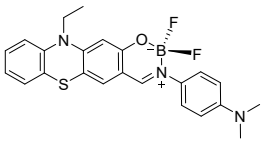

BPTZ4: A yellow solid was obtained in 95% yield (P: DCM =1: 5, *v*/*v*). **^{1}H NMR** (600 MHz, $CDCl_3$) δ/ppm = 8.06 (s, 1H), 7.40 (d, J = 9.0 Hz 2H), 7.19 – 7.16 (m, 1H), 7.10 – 7.08 (m, 1H), 7.03 (s, 1H), 6.99–6.95 (m, 2H), 6.72 (d, J = 9.0 Hz, 2H), 6.52 (s, 1H), 3.99–3.95 (m, 2H), 3.00 (s, 6H), 1.47 (t, J = 6.6 Hz, 3H). **^{13}C NMR** (150 MHz, $CDCl_3$) δ/ppm = 160.6, 156.9, 153.6, 150.6, 141.9, 131.9, 128.0, 127.7, 127.3, 124.0, 123.8, 123.1, 116.1, 114.9, 112.5, 103.9, 43.3, 40.6, 12.8. **HRMS** (ESI^+): calcd. for $C_{23}H_{22}BF_2N_3OS$: $[M + Na]^+$ = 460.1437, found: $[M + Na]^+$ = 460.1433.

Synthesis of BPTZ5

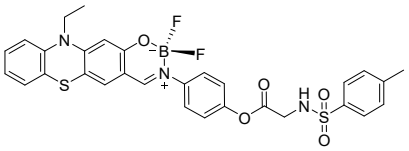

To a solution of compound **BPTZ3** (1 equiv) and *N*-*P*-Tosylglycine (1.5 equiv) in 10mL dry DCM in a 50 mL three-necked round-bottomed flask was added 4-dimethylaminopyridine (1 equiv) and dicyclohexylcarbodimide (1 equiv)[3]. In N_2 atmosphere protection, the solvent was stirred at room temperature for 12 h. The reaction mixture was extracted with DCM three times and washed with saturated sodium chloride aqueous solution. Organic layers were dried over $MgSO_4$ and evaporated under vacuum. The product was purified by silica gel chromatography. A red solid was obtained in 30% yield (DCM: MeOH =10: 1, *v*/*v*). **^{1}H NMR** (400 MHz, $CDCl_3$) δ/ppm = 8.05 (s, 1H), 7.79 (d, J = 7.6 Hz, 2H), 7.48 (d, J = 8.0 Hz, 2H), 7.36–7.32 (m, 2H), 7.20–7.16 (m, 1H), 7.08 (d, J = 7.6 Hz, 1H), 7.02–6.98 (m, 5H), 6.85 (d, J = 8.0 Hz, 1H), 6.46 (d, J = 8.4 Hz, 1H), 4.06 (d, J = 4.8 Hz, 2H), 3.96–3.94 (m, 2H), 2.43 (s, 3H), 1.45 (t, J = 6.4 Hz, 3H). **^{13}C NMR** (150 MHz, $CDCl_3$) δ/ppm = 167.6, 159.6, 154.7, 149.9, 144.3, 141.2, 140.7, 136.3, 130.1, 128.4, 127.5, 127.3, 124.7, 124.2, 124.0, 122.8, 122.4, 116.4, 116.3, 116.2, 115.4, 103.5, 44.5, 43.5, 21.7, 12.7. **HRMS** (ESI^+): calcd. for $[M-H]^-$ = 620.1291, found: $[M-H]^-$ = 620.1298.

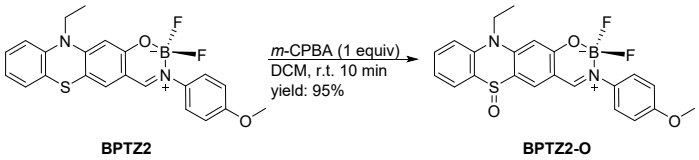

Scheme S2. Synthesis of **BPTZ2-O.**

To a 25 mL three-necked round-bottomed flask containing 5 mL dry DCM was added **BPTZ2** (1 equiv) and *m*-CPBA (1 equiv) in one portion. The mixture was stirred at room temperature for 10 min, and then extracted with DCM, and washed with sodium bicarbonate solution. Organic layers were evaporated under vacuum and washed with ether. A yellow solid was obtained in 95% yield. **^{1}H NMR** (400 MHz, $CDCl_3$) δ/ppm = 8.41 (s, 1H), 8.11 (s, 1H), 7.96 (d, J = 8.0 Hz, 1H), 7.69 (t, J = 7.6 Hz, 1H), 7.51 (d, J = 8.8 Hz, 3H), 7.36 (t, J = 7.2 Hz, 1H), 7.03–6.99 (m, 3H), 4.35–4.30 (m, 2H), 3.87 (s, 3H), 1.62 (t, J = 6.8 Hz, 3H). **^{13}C NMR** (150 MHz, $CDCl_3$) δ/ppm = 161.8, 160.4, 159.8, 145.5, 138.4, 137.2, 135.3, 133.7, 132.1, 131.0, 125.0, 124.6, 123.6, 118.8, 116.6, 114.9, 103.9, 55.8, 43.8, 12.0. **HRMS** (ESI^+): calcd. for $[M + H]^+$ = 441.1251, found: $[M + H]^+$ = 441.1270, calcd. for $[M + Na]^+$ = 463.1070, found: $[M + Na]^+$ = 463.1091.

3. Photophysical properties

Absorption spectra were tested using a Shimadzu UV-1750 spectrophotometer. Fluorescence spectra were measured on a FLUOROMAX-4 spectrophotometer, slit width = 2 nm for excitation

and emission. 10 mM probe stock solution was prepared with DMF as a solvent. Dilute the stock solution with DMF/PBS buffer (1: 4, *v*/*v*, pH = 7.4, 0.4% Tween 80). OCl^- was prepared by diluting commercial NaClO solutions with PBS (10 mM, pH = 7.4). The concentration of OCl^- was determined by UV analysis with the extinction coefficient at 292 nm (ε = 350 $M^{-1}cm^{-1}$). Analytes for selectivity investigation were prepared according to the reported literature.[4]

PL spectra addition: λ_{ex} = 420 nm for **BPTZ1**; λ_{ex} = 426 nm for **BPTZ2**; λ_{ex} = 412 nm for **BPTZ3**; λ_{ex} = 428 nm for **BPTZ4** and λ_{ex} = 415 nm for **BPTZ5**. The above excitation slit is 2 nm.

4. Cell experiments

4.1 Cell incubation

RAW264.7 cells were obtained from the American Type Culture Collection (ATCC). The cells were cultured in RPMI-1640 medium supplemented with 10% fetal bovine serum, penicillin (100 units/mL), streptomycin (100 mg/mL), and 5% CO_2 at 37°C. The cells were maintained in an exponential growth phase by periodic subcultivation. The cell density was determined using a hemocytometer, and this was performed prior to any experiments.

4.2 In vitro Cytotoxicity

Rat pheochromocytoma (PC12) cells, human Embryonic Kidney 293T (293T) cells and human brain astroblastoma (U87MG) cells were incubated in 96 well plates, next treated with various concentrations of **BPTZ5** (0, 1, 2, 5, 10, 20, 30, 50 μM, in 200 μL DMEM (containing 10% FBS and 1% DMSO)). The experimental group and control group were incubated at 37℃, 5% carbon dioxide and 95% air atmosphere for 48 h. Then 20 μL MTT solution (5.0 mg/mL) was added to each hole. After 4 h incubation under the same conditions, the supernatant was removed and 150 μL DMSO was added. The cells were shaken at low speed for 10 min, and the absorbance at 490 nm was measured with a microplate reader (Synergy 2, BioTek Instruments Inc). Cell survival rate was determined by $A/A_0 \times 100\%$ (A_0 and A respectively are the absorbance of the control group and experimental group).

4.3 Cell imaging

Mouse leukemia cellsof momocyte macrophage (RAW264.7) cells were divided into five groups.

1) RAW264.7 cells were treated with 5 μM **BPTZ5** and incubated for 30 minutes.
2) RAW264.7 cells were pretreated with ABH (250 μM) for 4 h, then 5 μM **BPTZ5** was added and incubated for 30 minutes.
3) RAW264.7 cells were pretreated with ABH (250 μM) for 4 h. Next, 20 $\mu g \cdot mL^{-1}$ LPS and 5 $\mu g \cdot mL^{-1}$ PMA were added and incubated for 12 h. Then 5 μM **BPTZ5** was added and incubated for 30 minutes.
4) RAW264.7 cells were pretreated with ABH (250 μM) 4 h. Next, 80 μM NaClO was added and incubated for 4 h. Then 5 μM **BPTZ5** was added and incubated for 30 minutes.
5) RAW264.7 cells were pretreated with ABH (250 μM) for 4 h. Next, 20 $\mu g \cdot mL^{-1}$ LPS and 5 $\mu g \cdot mL^{-1}$ PMA were added and incubated for 12 h. Then ABH (250 μM) was added and incubated for 4 h. Finally, 5 μM **BPTZ5** was added and incubated for 30 minutes.

The cell samples were imaged on confocal microscopy (Zeiss LSM710) with the excitation at 415 nm (emission 450–580 nm) and 415 nm (emission 590–700 nm), respectively.

5. Supplementary tables and figures

Table S1. Photophysical data of **BPTZ1-5** in DCM.

Cpd	λ_{abs} (nm)	ε (M^{-1} cm^{-1})	λ_{em} (nm)	Φ_f(%)
BPTZ1	312/458	26000/21000	634	16.1%
BPTZ2	326/458	23000/24000	629	24.5%
BPTZ3	325/457	22000/22000	628	21.6%
BPTZ4	288/475	22000/34000	619	25.1%
BPTZ5	313/460	22000/21000	634	16.2%

[a]Data obtained at 343 K. [b]Determined using coumarin 6 (Φ_f = 80%) as the reference.

Table S2. Photophysical data of **BPTZ1** in different solvents.

Solvent	λ_{abs} (nm)	ε (M^{-1} cm^{-1})	λ_{em} (nm)
Toluene	312/454	24000/20000	603
Dichloromethane	312/458	26000/21000	634
Tetrahydrofuran	312/447	27000/20000	620
Ethyl acetate	310/442	27000/21000	618
1,4-Dioxane	312/448	26000/20000	610
Acetonitrile	307/446	14000/19000	645
N, N-dimethylformamide	310/448	24000/19000	646
Dimethyl sulfoxide	312/449	25000/17000	650

Table S3. Photophysical data of **BPTZ2** in different solvents.

Solvent	λ_{abs} (nm)	ε (M^{-1} cm^{-1})	λ_{em} (nm)
Toluene	326/454	20000/22000	597
Dichloromethane	326/458	23000/25000	629
Tetrahydrofuran	324/447	27000/27000	611
Ethyl acetate	322/443	22000/23000	608
1,4-Dioxane	325/448	22000/22000	604
Acetonitrile	319/446	14000/22000	637
N, N-dimethylformamide	320/448	20000/21000	638
Dimethyl sulfoxide	325/449	22000/21000	645

Table S4. Photophysical data of **BPTZ3** in different solvents.

Solvent	λ_{abs} (nm)	ε (M^{-1} cm^{-1})	λ_{em} (nm)
Toluene	323/451	16000/21000	594
Dichloromethane	325/457	21000/23000	628
Tetrahydrofuran	325/448	19000/21000	608
Ethyl acetate	320/442	17000/20000	606
1,4-Dioxane	321/448	17000/21000	602
Acetonitrile	324/445	12000/20000	638
N, N-dimethylformamide	326/447	20000/21000	633
Dimethyl sulfoxide	326/449	18000/20000	640

Table S5. Photophysical data of **BPTZ4** in different solvents.

Solvent	λ_{abs} (nm)	ε (M^{-1} cm^{-1})	λ_{em} (nm)
Toluene	309/469	15000/31000	591
Dichloromethane	288/475	22000/34000	619
Tetrahydrofuran	312/463	16000/32000	602
Ethyl acetate	310/459	15000/32000	600
1,4-Dioxane	313/463	14000/30000	600
Acetonitrile	304/463	5000/30000	628
N, N-dimethylformamide	310/467	24000/30000	626
Dimethyl sulfoxide	288/469	21000/30000	629

Table S6. Photophysical data of **BPTZ5** in different solvents.

Solvent	λ_{abs} (nm)	ε (M^{-1} cm^{-1})	λ_{em} (nm)
Toluene	315/455	18000/20000	605
Dichloromethane	313/460	22000/21000	634
Tetrahydrofuran	312/449	24000/20000	616
Ethyl acetate	312/444	25000/22000	614
1,4-Dioxane	313/449	24000/20000	616
Acetonitrile	313/447	17000/20000	643
N, N-dimethylformamide	313/448	20000/21000	641
Dimethyl sulfoxide	313/451	18000/19000	645

Table S7. Summary of reported fluorescent probes for OCl^-.

Ref. in SI	Probe	$\lambda_{ex}\lambda_{em}$ (nm)	Detection limit	Application
5	**TQE-SQ5** 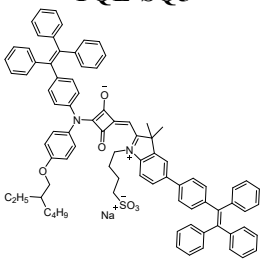	380 485/643	5.6 nM	Living cells
6	**TQE-SQ3** 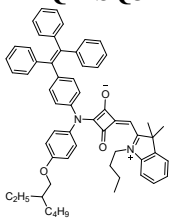	529 650	105 nM	Living cells
7	**PDC** 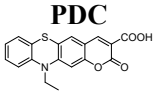	415 503	16.1 nM	Living cells and BALB/c mice with the OA model
8	**BPC1** 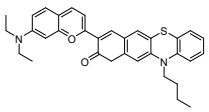	380 485	13 nM	Living cells and zebrafish
9	**PBC** 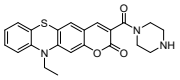	385 520	6.82 nM	Living cells
10	**PZ-HA** 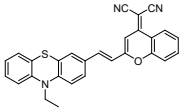	450 650	0.72 μM	Living cells and zebrafish
11	**HCP** 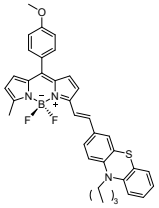	590 615	4.1 nM	Living cells
12	**Pz-Py** 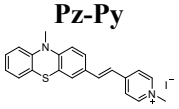	400 562	17.9 nM	Living cells and living mice

13	**Cou-Lyso** 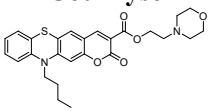	440 535/610	0.58 μM	Living cells and zebrafish
14	**PI-Py** 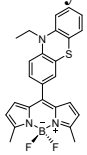	500 515	1.7 nM	Living cells
15	**PTC** 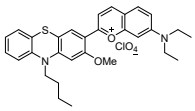	520 627	7.74 nM	Living cells and zebrafish
16	**PHPQ** 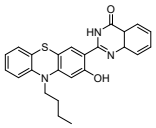	405 437/535	15 nM	Living cells and zebrafish
17	**PPS** 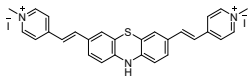	408 537	24 nM	Living cells and RA mouse model
18	**ClO-1** 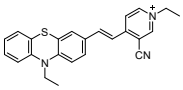	450 562/635	1.12 nM	Living cells
19	**TJ2** 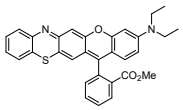	500 594/730	2.3 nM	Living cells
20	**ERC** 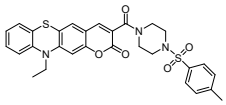	390 503/609	0.44 μM	Living cells
21	**P1** 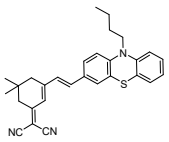	480 620	42 nM	Living cells and zebrafish
22	**L1** 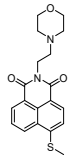	405 505	0.674 μM	Living cells
Our work	**BPTZ5** 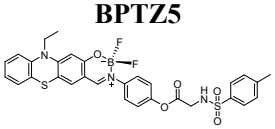	415 515/630	21.1 nm	Living cells

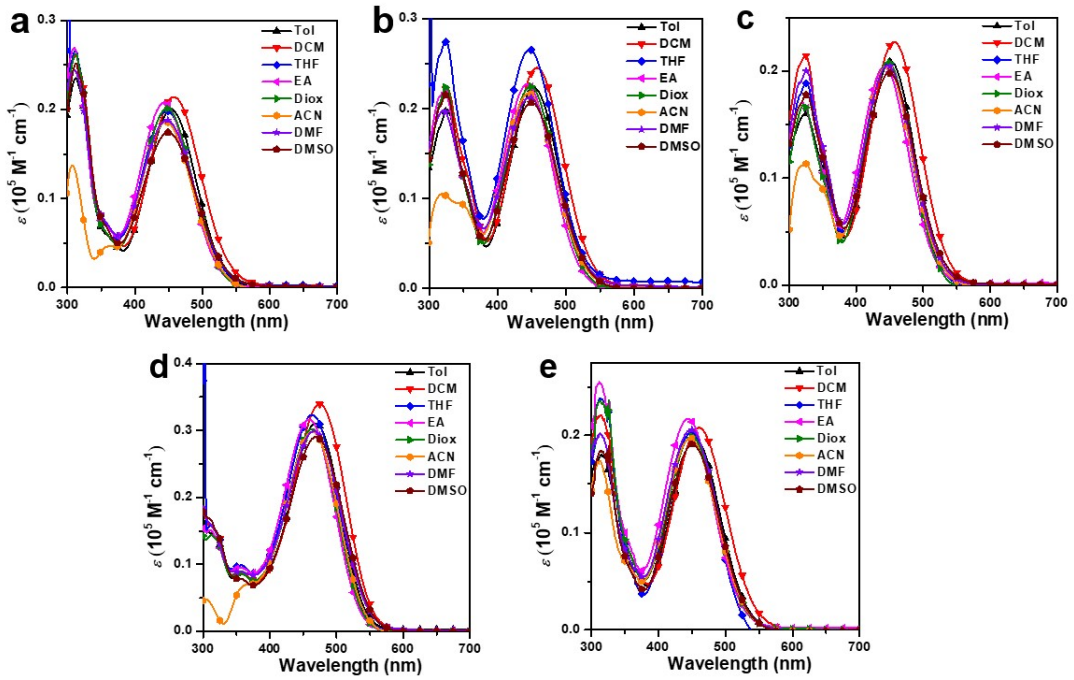

Figure S1. Absorption spectra of **BPTZ1-5** (10 μM) in various solvents with different polarity.

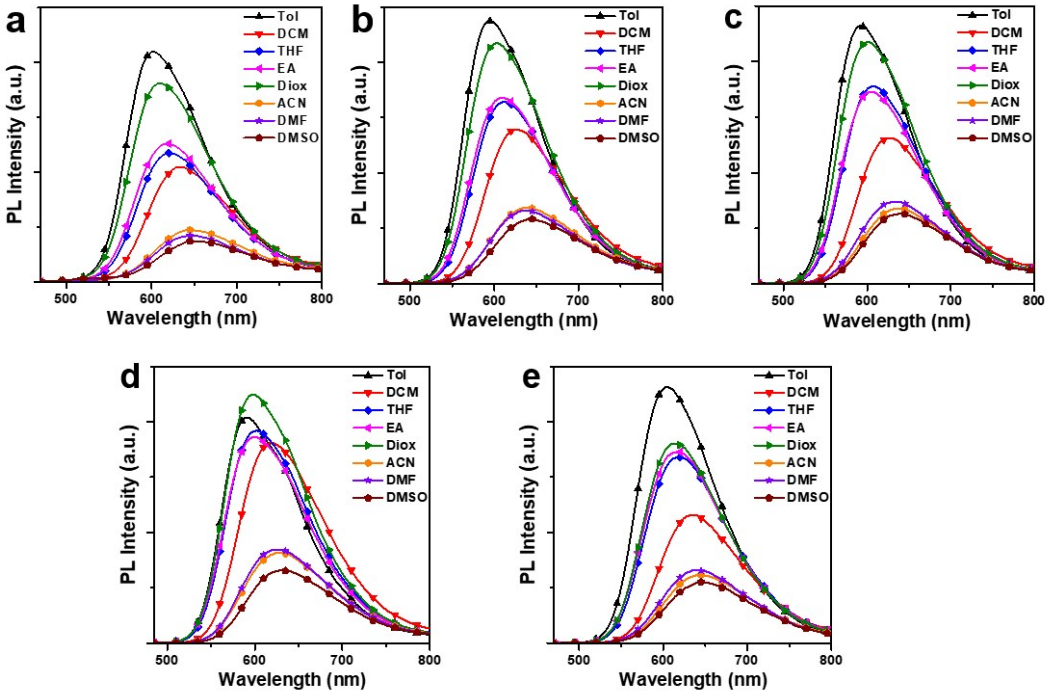

Figure S2. Emission spectra of **BPTZ1-5** (10 μM) in various solvents.

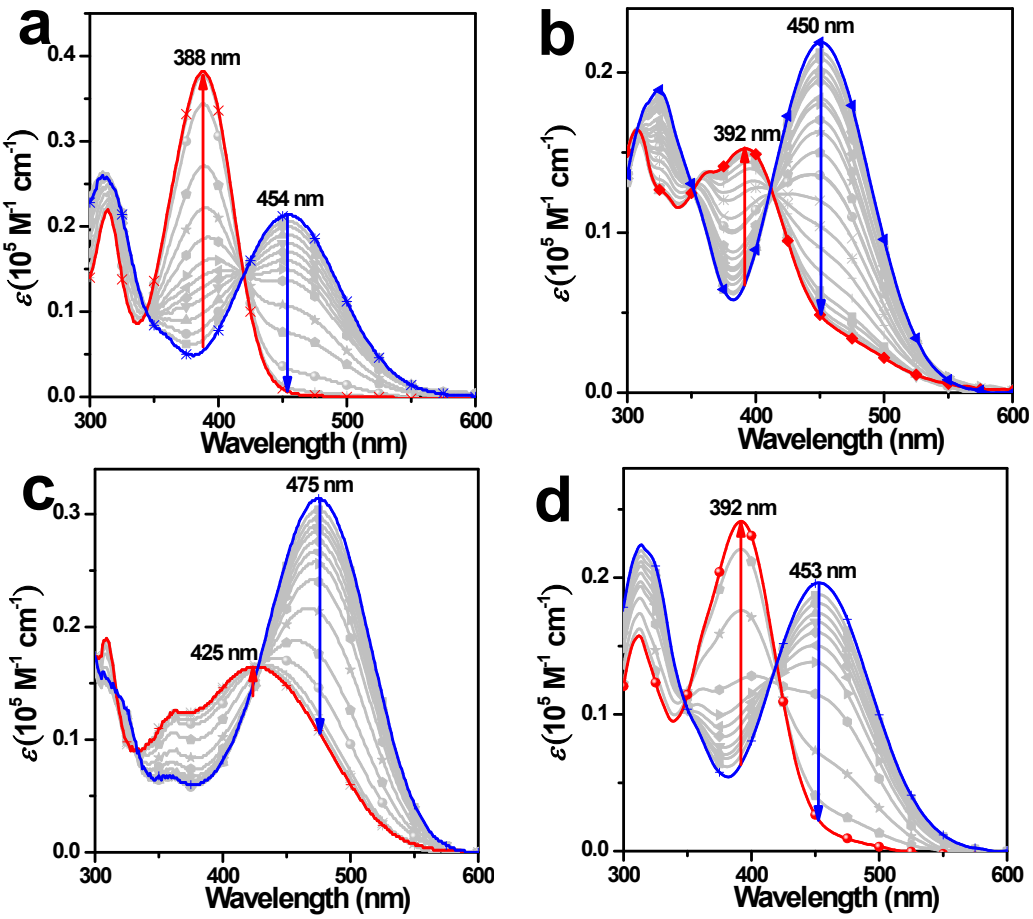

Figure S3. Absorption spectra changes of (a) **BPTZ1**, (b) **BPTZ3**, (c) **BPTZ4**, (d) **BPTZ5** (5 μM) in the presence of increasing concentrations of OCl^- in DMF/PBS buffer at room temperature.

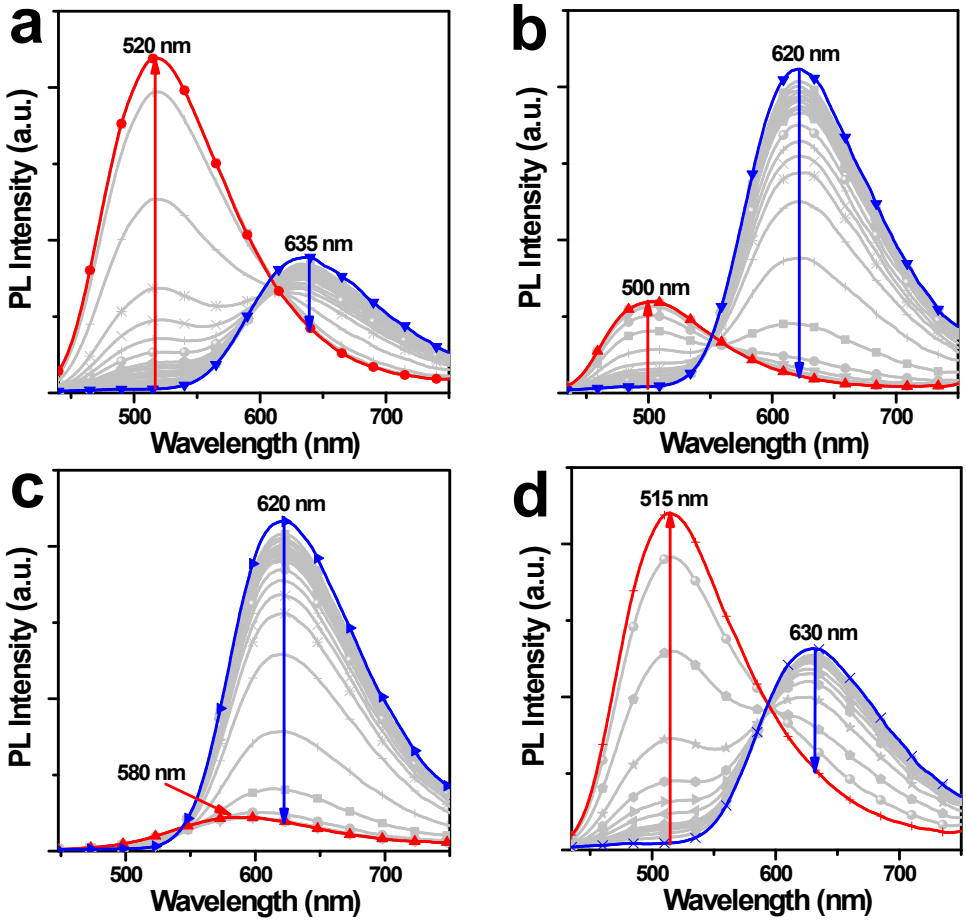

Figure S4. Emission spectra changes of (a) **BPTZ1**, (b) **BPTZ3**, (c) **BPTZ4**, (d) **BPTZ5** (5 μM) in the presence of increasing concentrations of OCl^- in DMF/PBS buffer at room temperature.

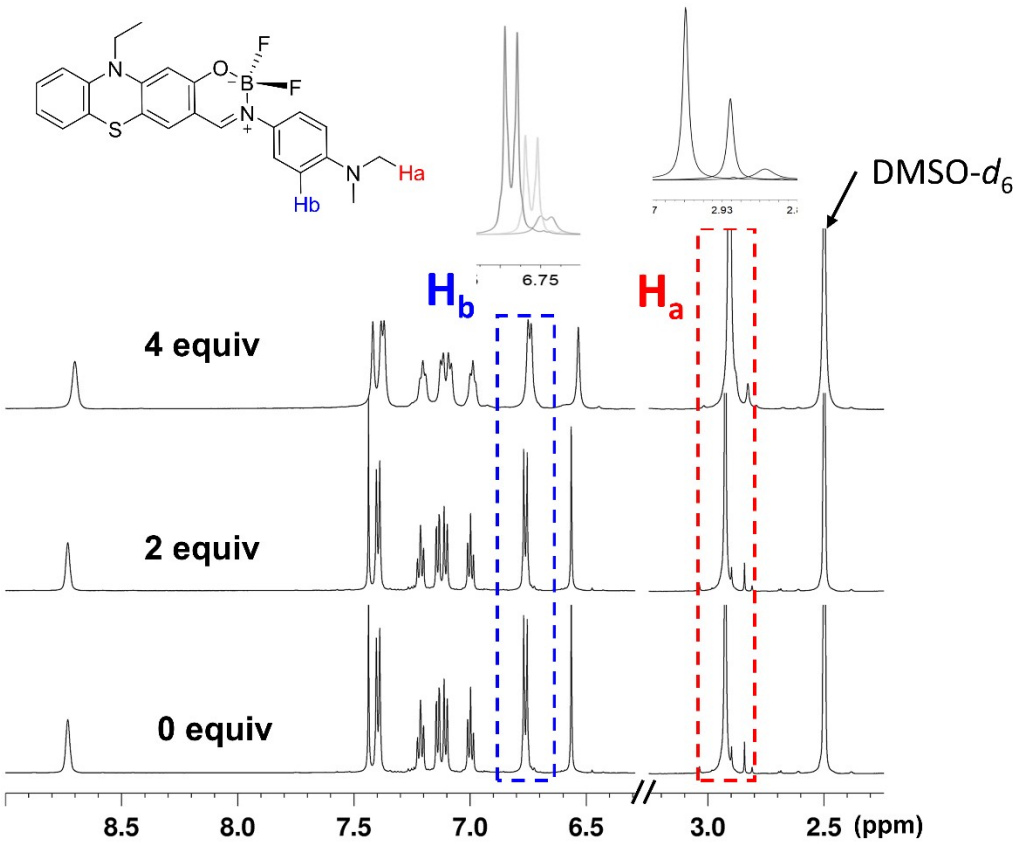

Figure S5. The ^{1}H NMR spectra of **BPTZ4** (20 mM) in the presence of different concentrations of OCl^- in DMSO-d_6.

We carried out the ^{1}H NMR titration experiments to confirm that the dimethylaminophenyl group was oxidized after the addition of hypochlorite.

As shown in Figure S5, the addition of hypochlorite to the solution of **BTPZ4** caused a distinct down-field shift for the signals of the protons in the dimethylamino group (H_a) and the phenyl ring (H_b), which suggests that the dimethylaminophenyl group was oxidized by hypochlorite. However, the oxidation products cannot be separated due to their highly unstable nature.

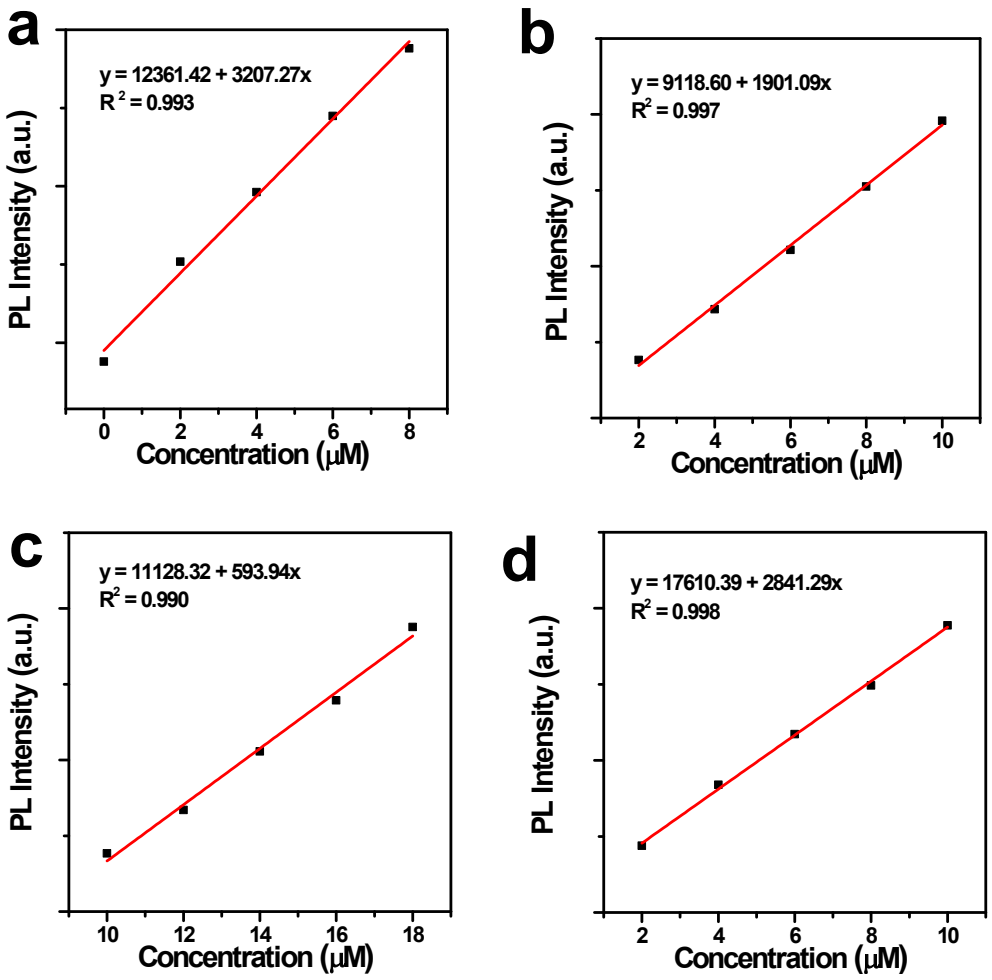

Figure S6. Calibration curve of emission intensity of (a) **BPTZ1** at 520 nm, (b) **BPTZ2** at 500 nm, (c) **BPTZ3** at 500 nm, (d) **BPTZ5** (5 μM) at 515 nm.

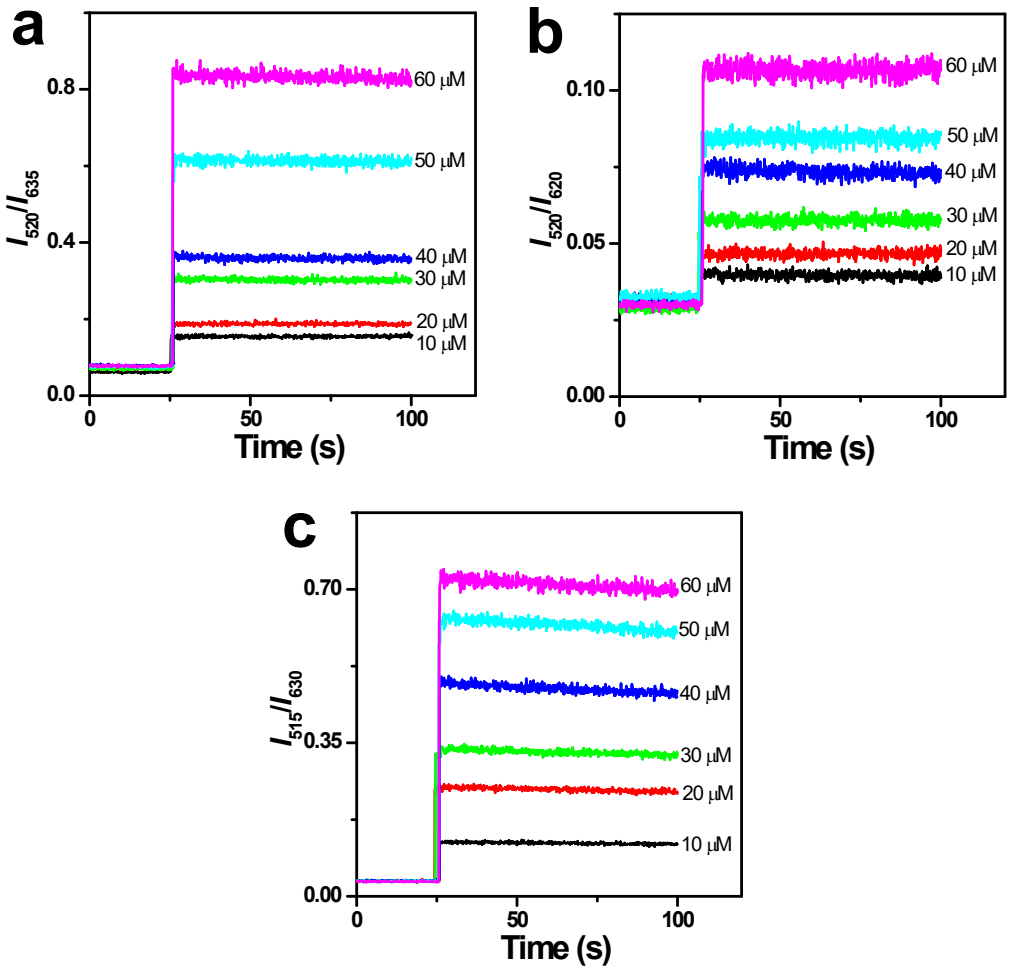

Figure S7. Time-dependent fluorescence intensity ratio of (a) **BPTZ1**, (b) **BPTZ3**, (c) **BPTZ5** (5 μM) with various concentrations of OCl^- in DMF/PBS buffer at room temperature.

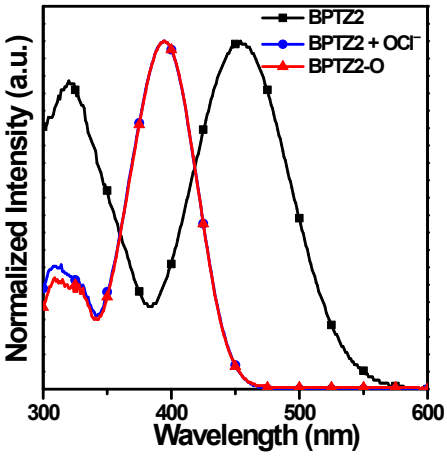

Figure S8. Absorption spectral of **BPTZ2** and **BPTZ2** treated with OCl^- in DMF/PBS buffer at room temperature. (The black line is **BPTZ2** (5 μM), the blue line is **BPTZ2** (5 μM) treated with OCl^- (120 μM) for 2 min, and the red line is **BPTZ2-O** which is the corresponding product.

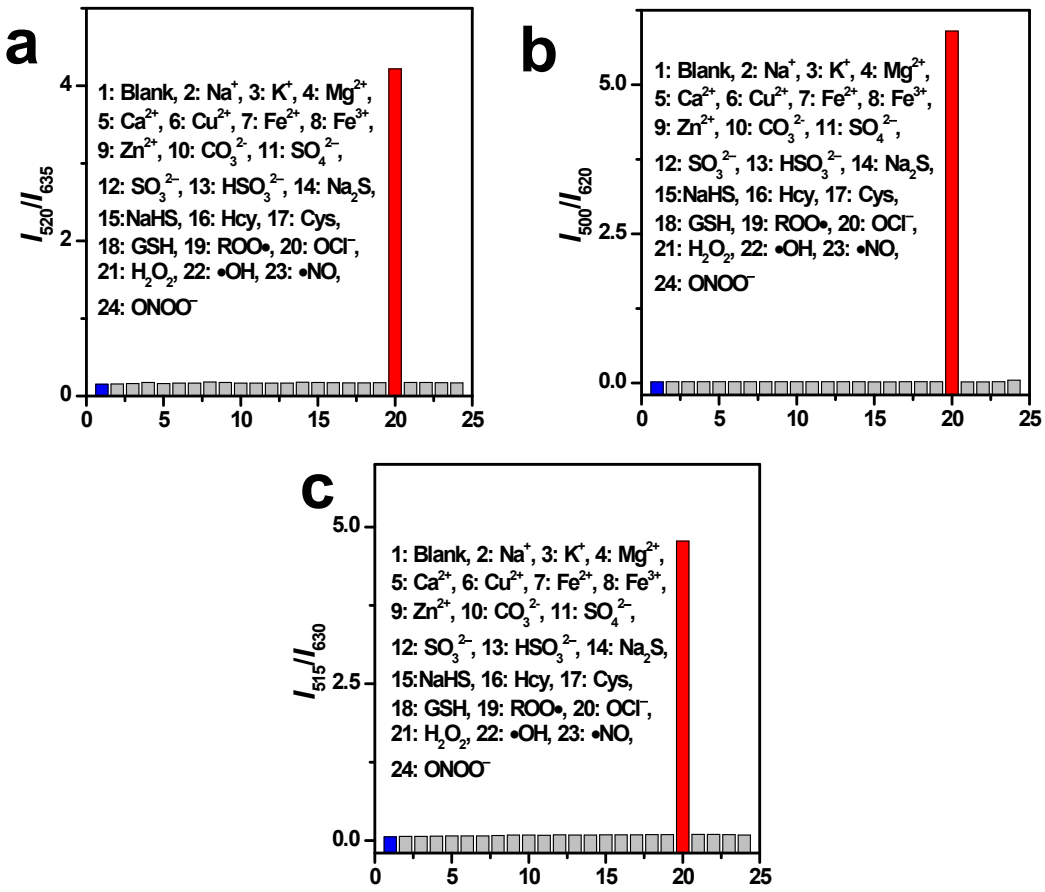

Figure S9. The fluorescence intensity ratio of (a) **BPTZ1**, (b) **BPTZ3**, (c) **BPTZ5** (5 μM) with 150 μM OCl^- and other analysts in DMF/PBS buffer at room temperature.

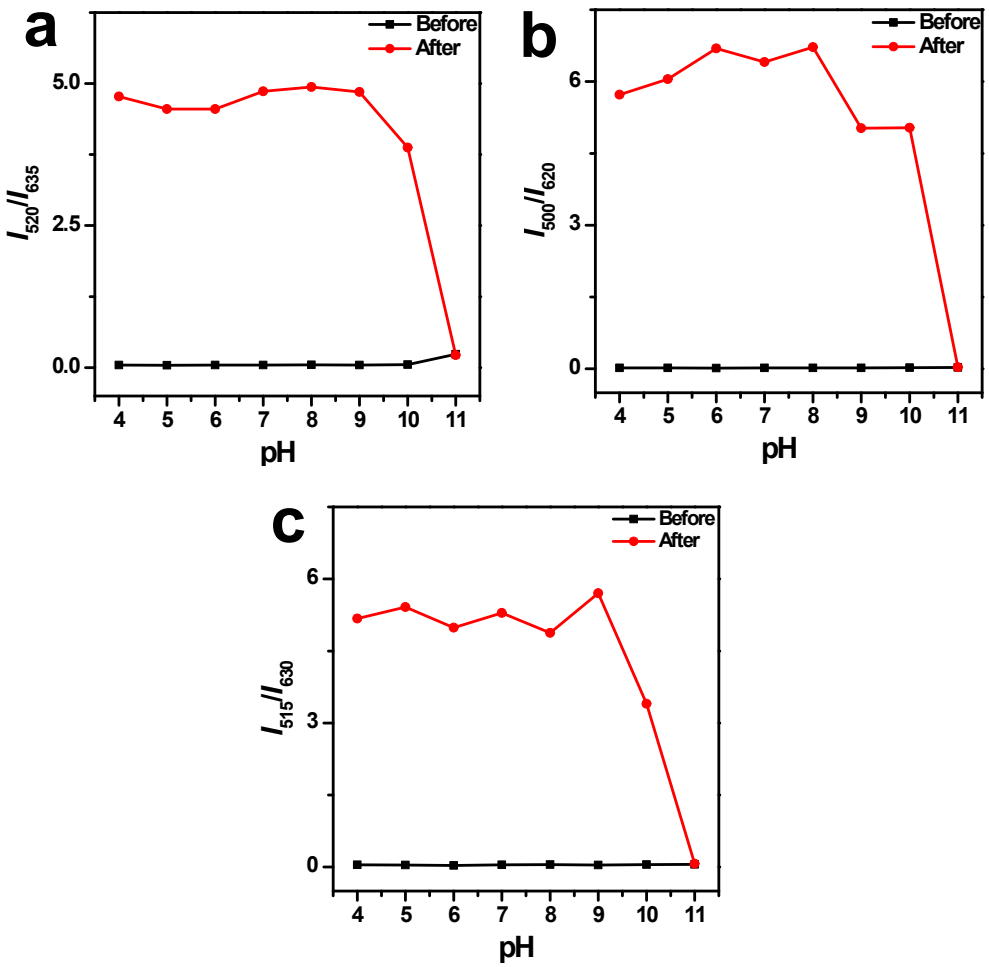

Figure S10. Effects of pH on the fluorescence intensity ratio of (a) **BPTZ1**, (b) **BPTZ3**, (c) **BPTZ5** (5 μM) with 150 μM OCl^- in DMF-water solution at room temperature.

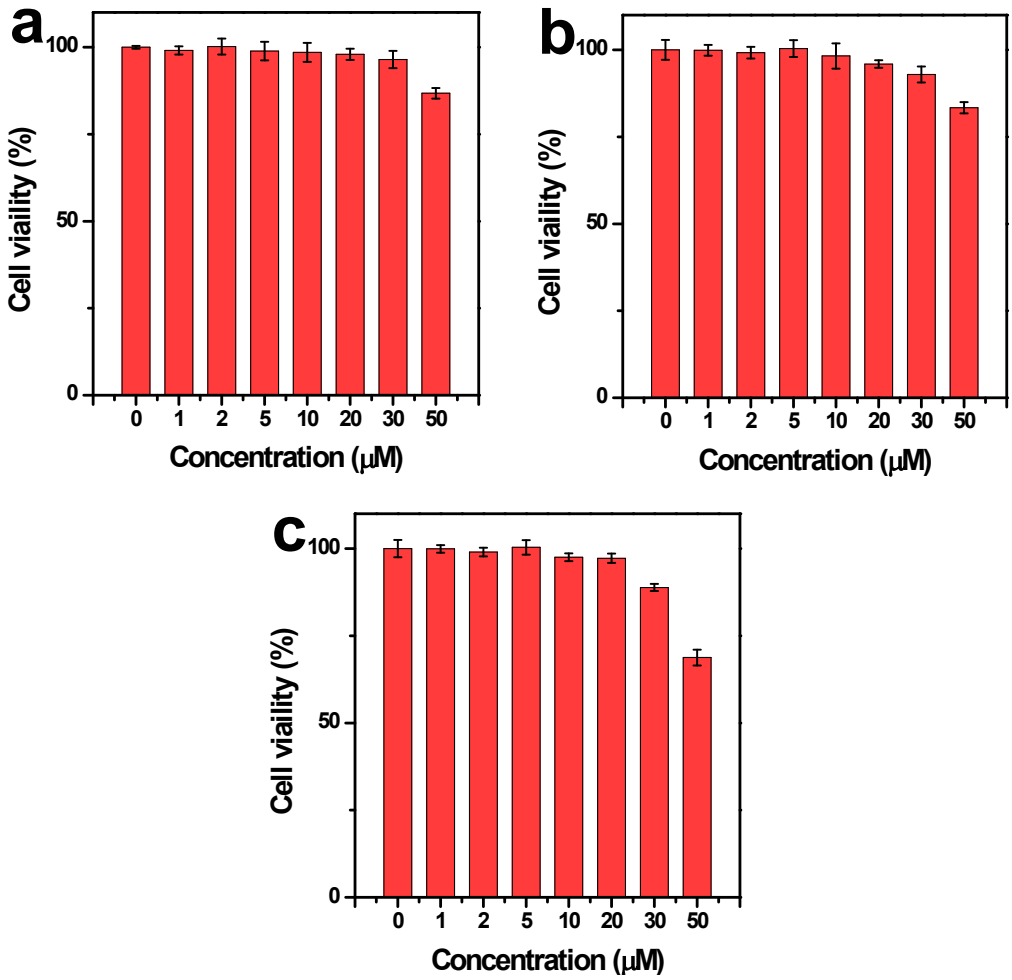

Figure S11. Cell viability of (a) PC12 (b) 293T (c) U87MG cells incubated with **BPTZ5** at various concentrations. Bars represent mean ± s.d. derived from n = 6 independent experiments.

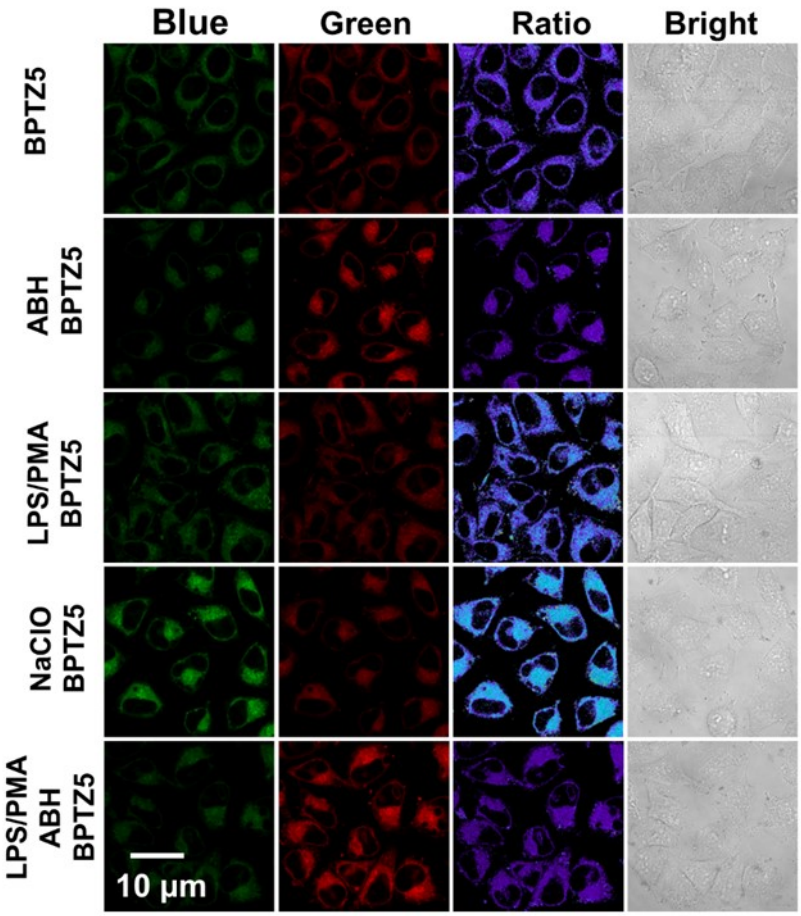

Figure S12. Confocal fluorescence images of **BPTZ5** in RAW264.7 cells under different conditions. **BPTZ5** group: cells were incubated with **BPTZ5** (5 μM, 30 min), then imaged; ABH + **BPTZ5** group: cells were pretreated with OCl^- scavenger ABH (250 μM, 4 h), next incubated with **BPTZ5** (5 μM, 30 min), then imaged; LPS + PMA + **BPTZ5** group: cells were pretreated with OCl^- scavenger ABH (250 μM, 4 h), next treated with LPS (5 μg·mL^{-1}) and PMA (5 μg·mL^{-1}) for 12 h, then incubated with **BPTZ5** (5 μM, 30 min) and imaged; NaClO + **BPTZ5** group: cells were pretreated with OCl^- scavenger ABH (250 μM, 4 h), next treated with NaClO (20 μM , 4 h), then incubated with **BPTZ5** (5 μM, 30 min) and imaged; LPS + PMA + ABH + **BPTZ5** group: cells were pretreated with OCl^- scavenger ABH (250 μM, 4 h), next treated with LPS (5 μg·mL^{-1}) and PMA (5 μg·mL^{-1}) for 12 h, then treated with ABH (250 μM, 4 h), finally incubated with **BPTZ5** (5 μM, 30 min) and imaged. Scale bar: 10 μM. (Blue channels: λ_{ex} = 415 nm, λ_{em} = 450–580 nm. Green channels: λ_{ex} = 415 nm, λ_{em} = 590–700 nm. Ratio: I_{blue}/I_{green})

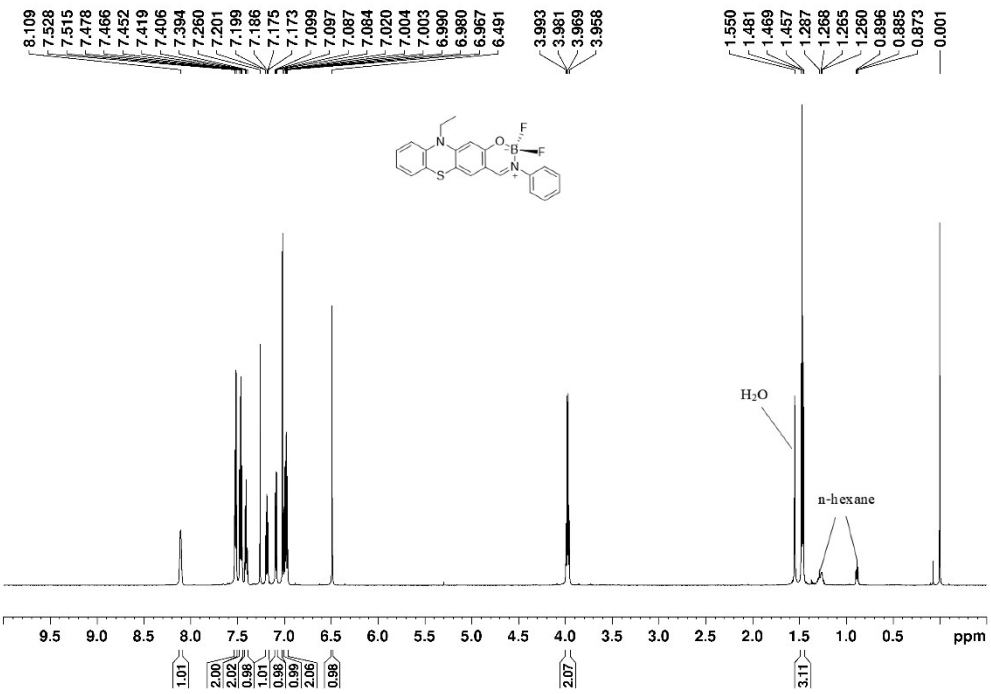

Figure S13. ^{1}H NMR spectrum of **BPTZ1** in $CDCl_3$.

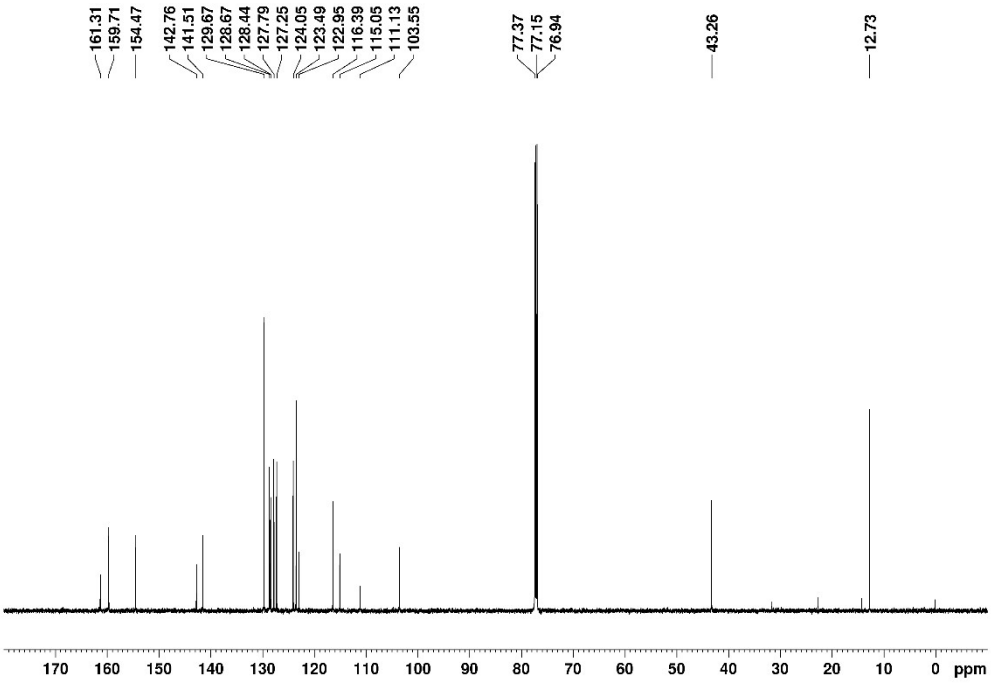

Figure S14. ^{13}C NMR spectrum of **BPTZ1** in $CDCl_3$.

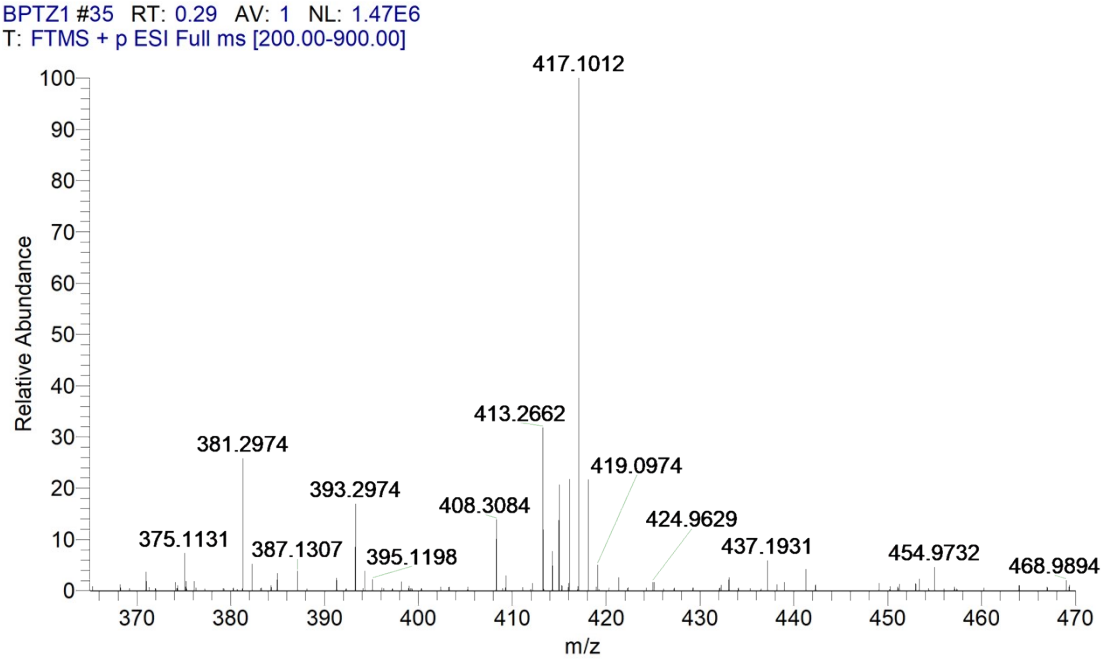

Figure S15. HRMS spectrum of **BPTZ1**.

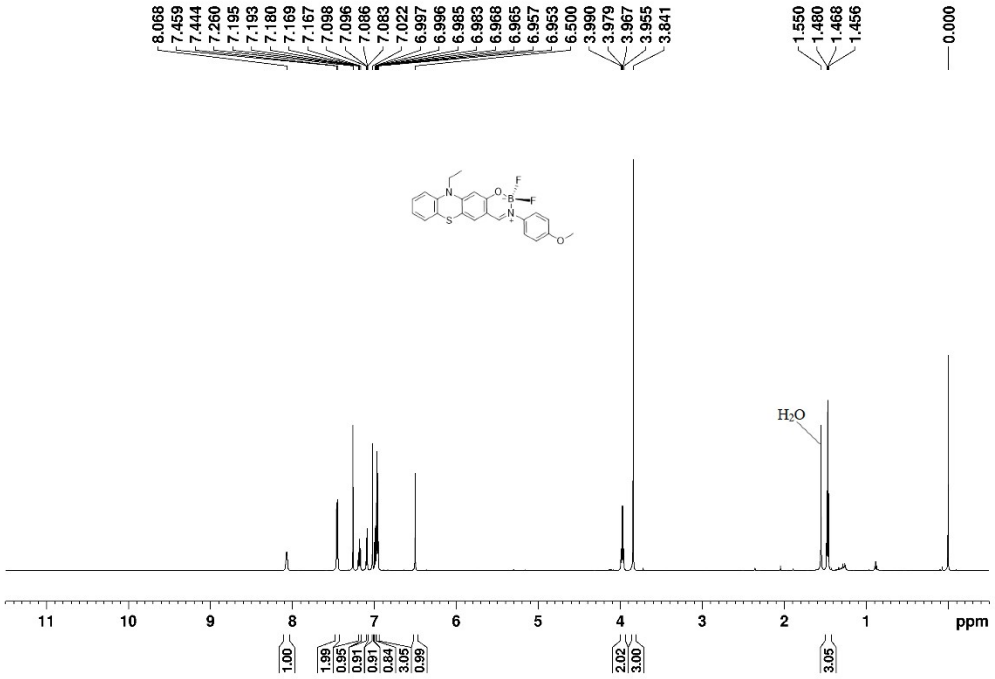

Figure S16. ^{1}H NMR spectrum of **BPTZ2** in $CDCl_3$.

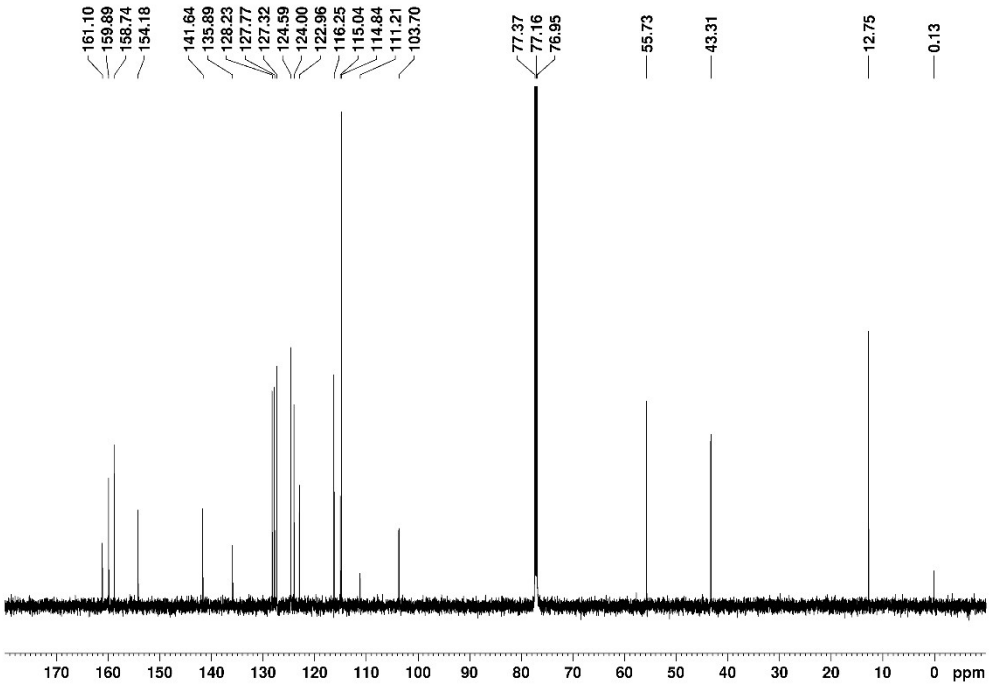

Figure S17. ^{13}C NMR spectrum of **BPTZ2** in $CDCl_3$.

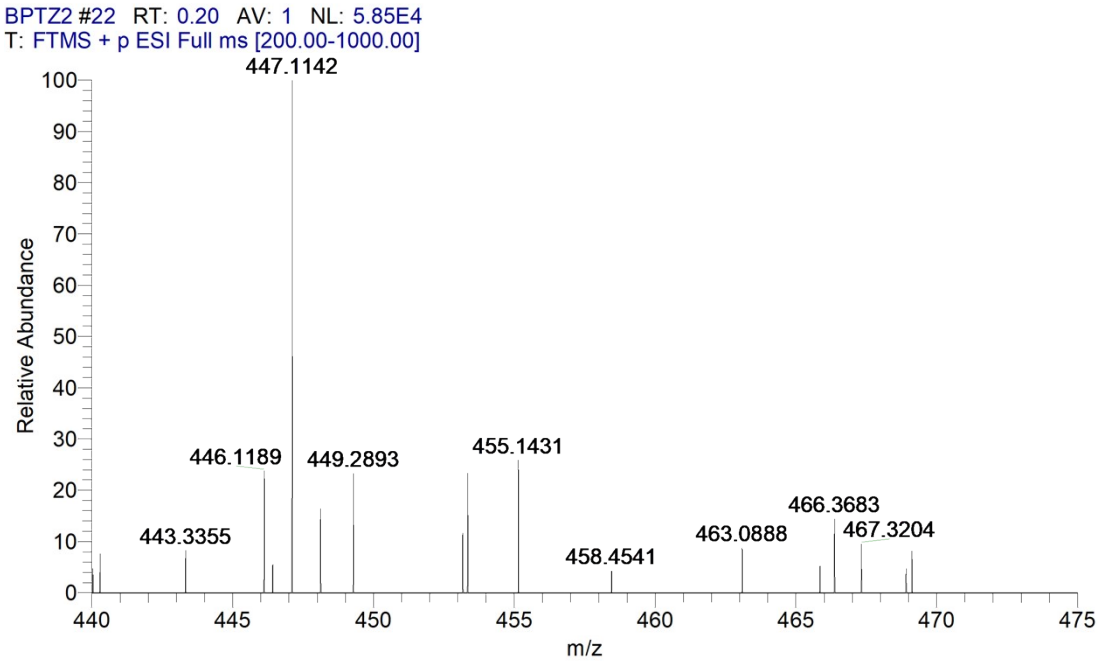

Figure S18. HRMS spectrum of **BPTZ2**.

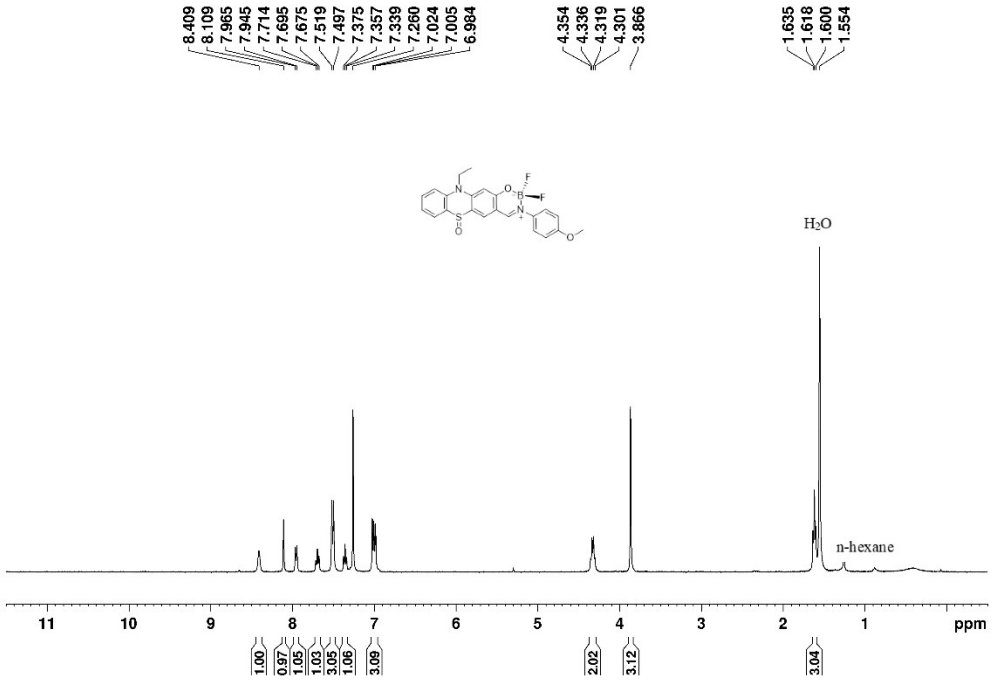

Figure S19. ^{1}H NMR spectrum of **BPTZ2-O** in $CDCl_3$.

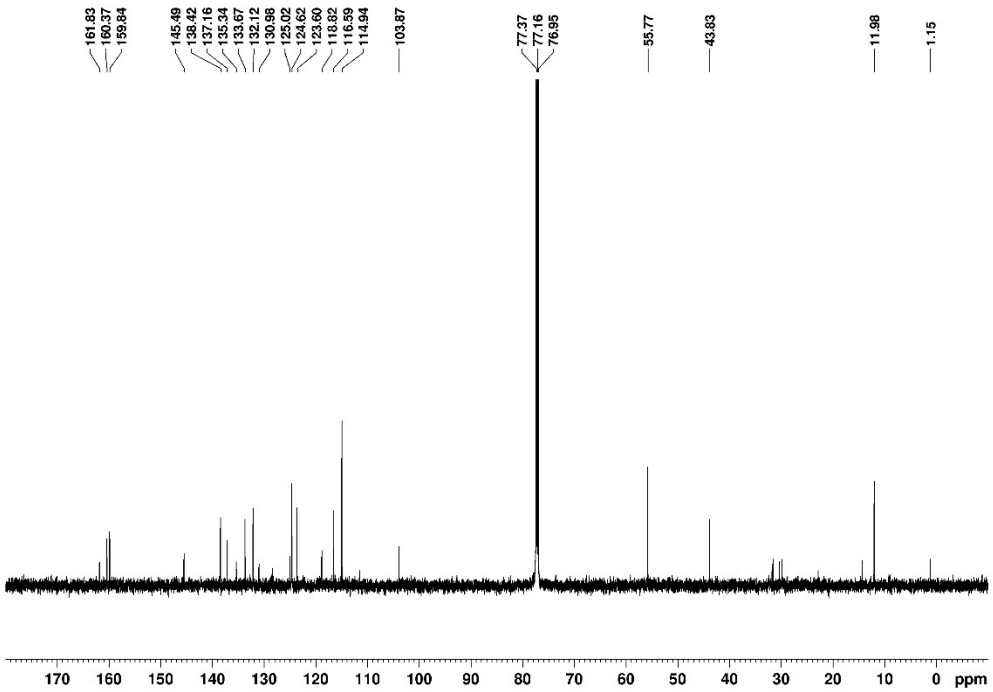

Figure S20. ^{13}C NMR spectrum of **BPTZ2-O** in $CDCl_3$.

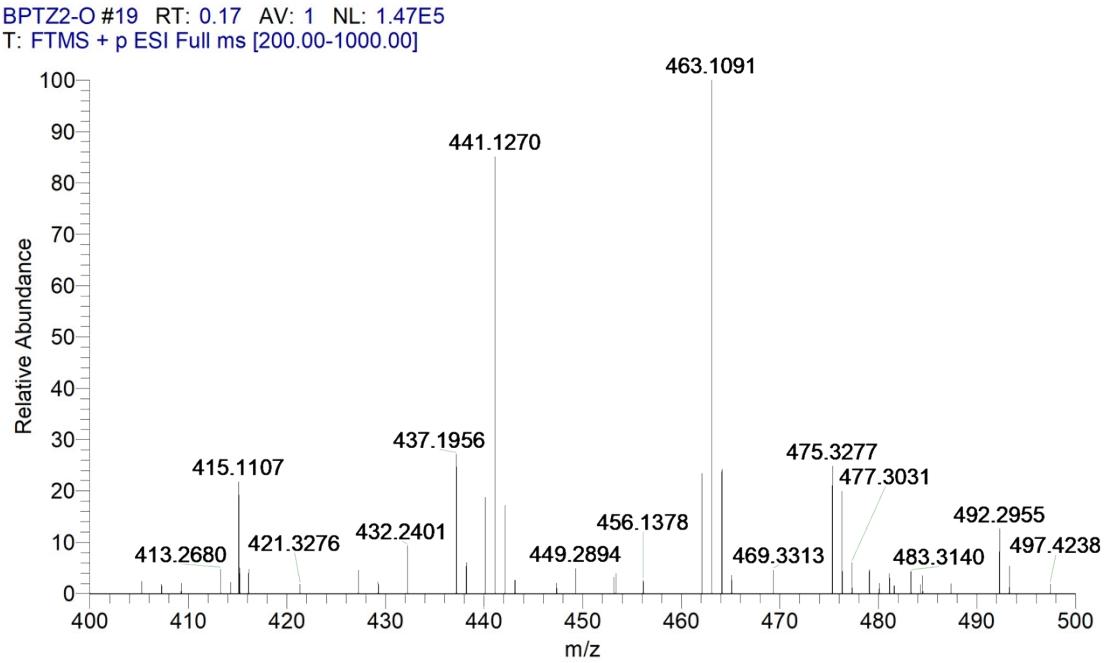

Figure S21. HRMS spectrum of **BPTZ2-O**.

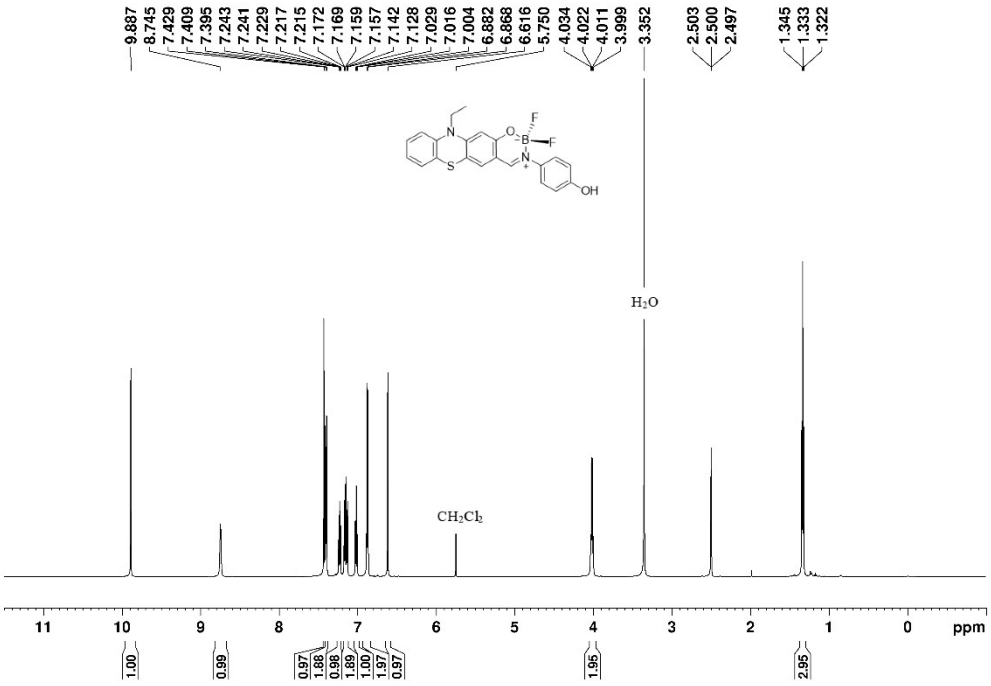

Figure S22. ^{1}H NMR spectrum of **BPTZ3** in DMSO.

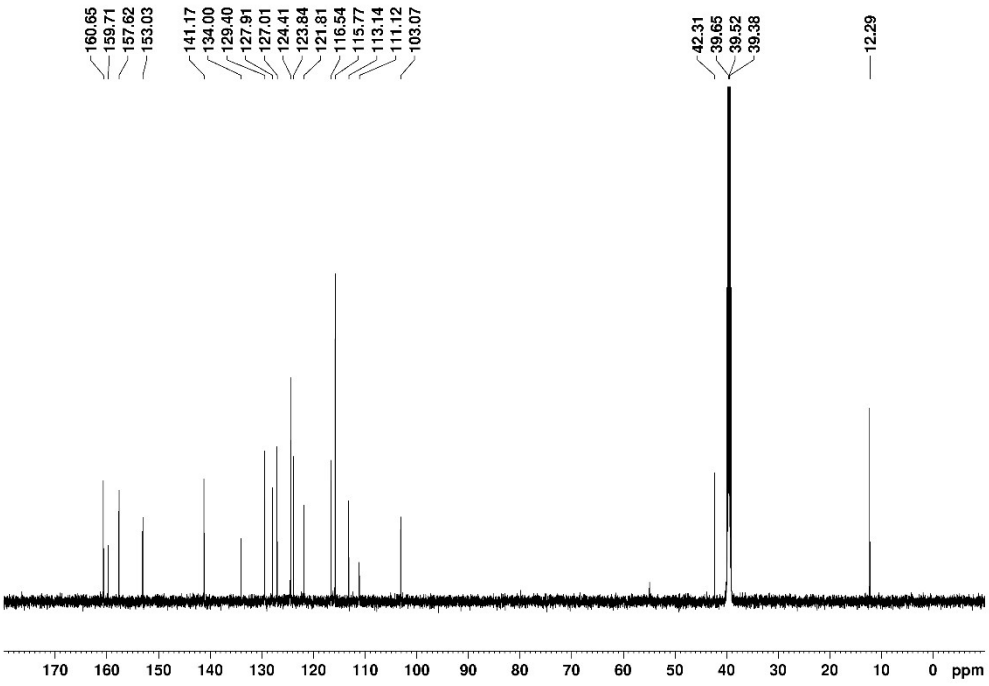

Figure S23. ^{13}C NMR spectrum of **BPTZ3** in DMSO.

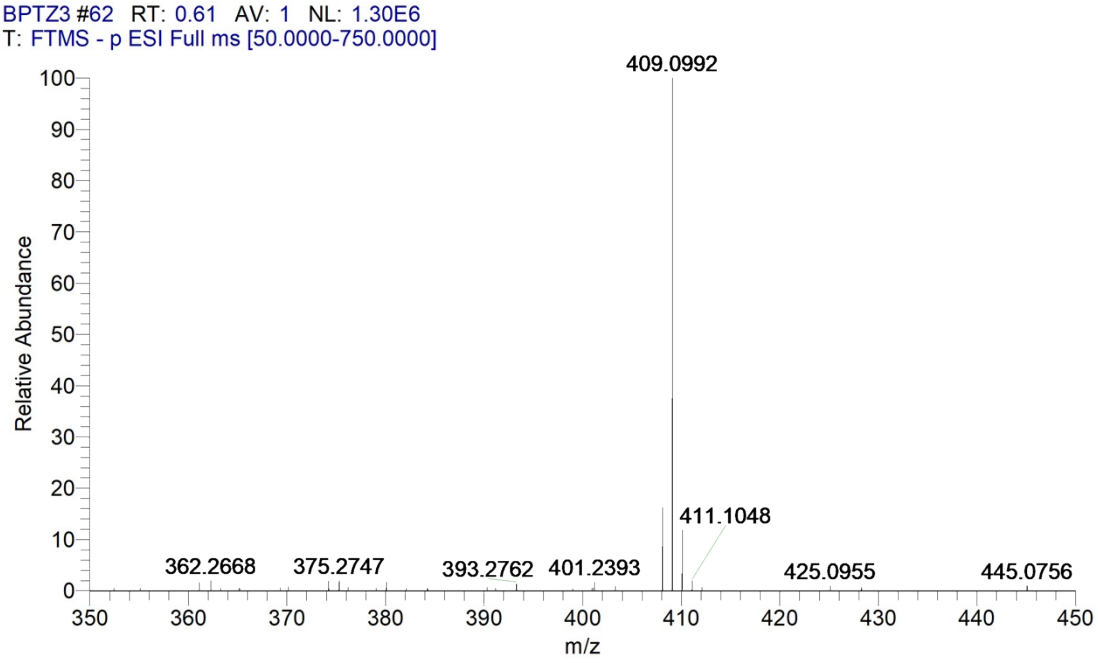

Figure S24. HRMS spectrum of **BPTZ3**.

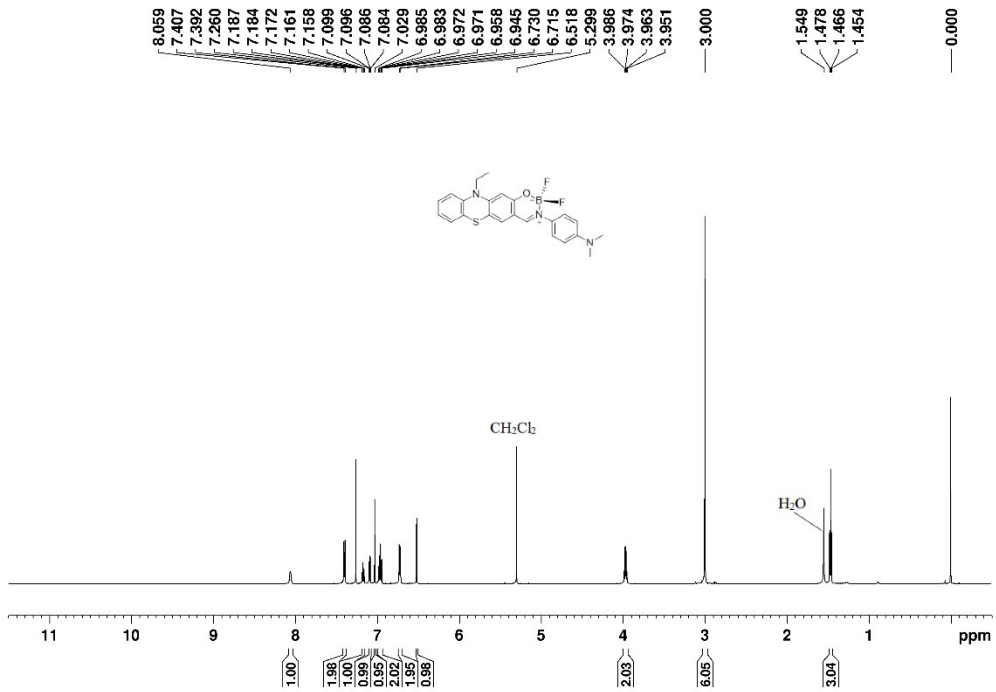

Figure S25. ^{1}H NMR spectrum of **BPTZ4** in $CDCl_3$.

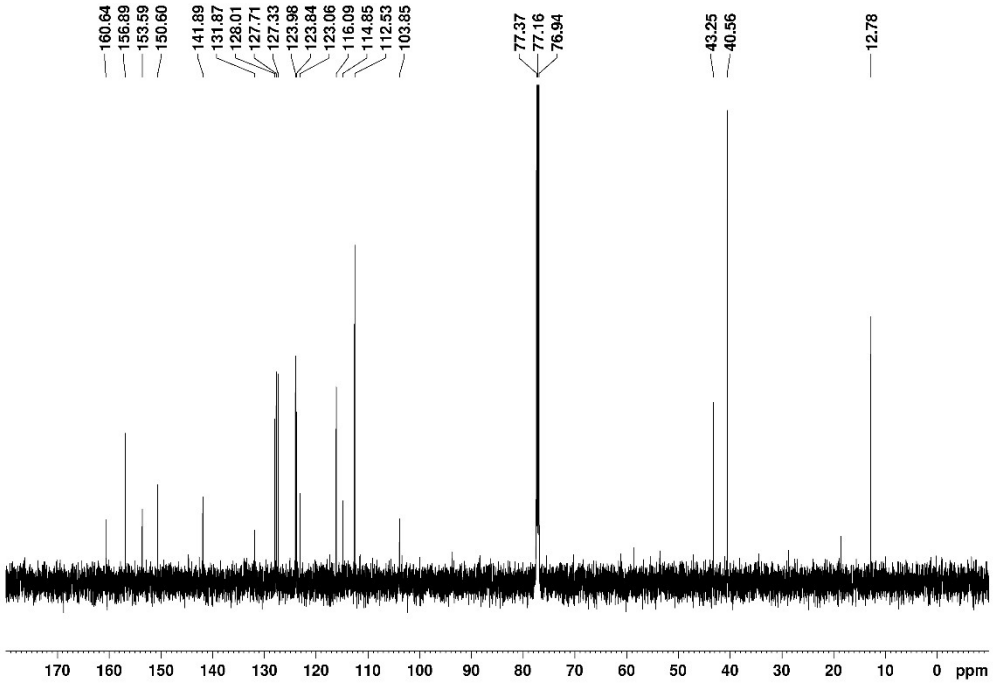

Figure S26. ^{13}C NMR spectrum of **BPTZ4** in $CDCl_3$.

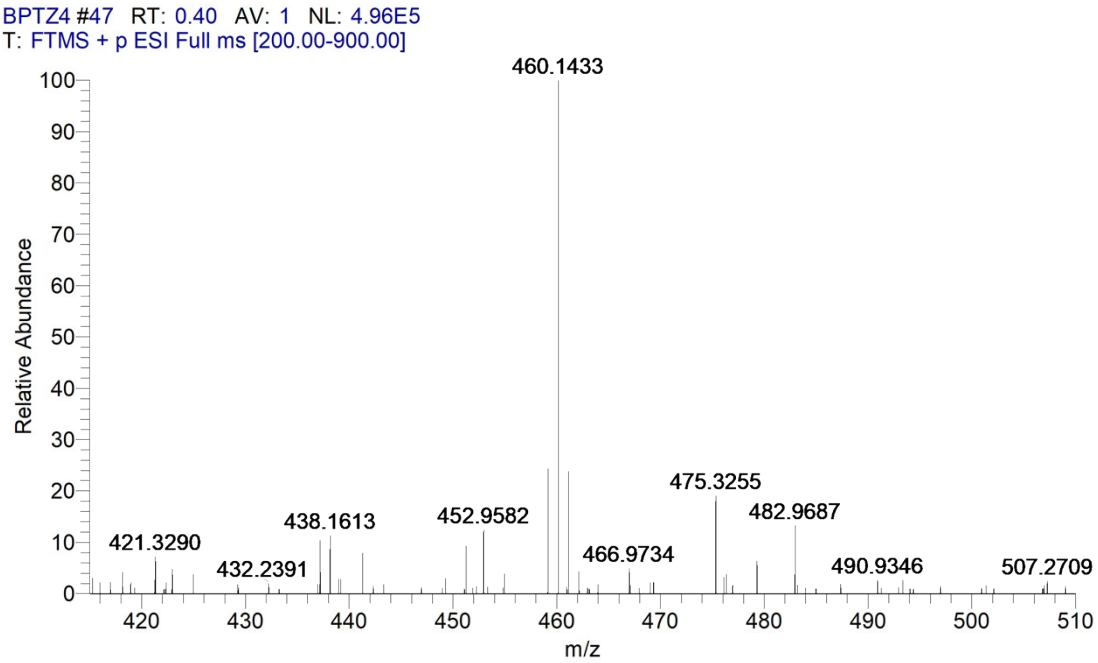

Figure S27. HRMS spectrum of **BPTZ4**.

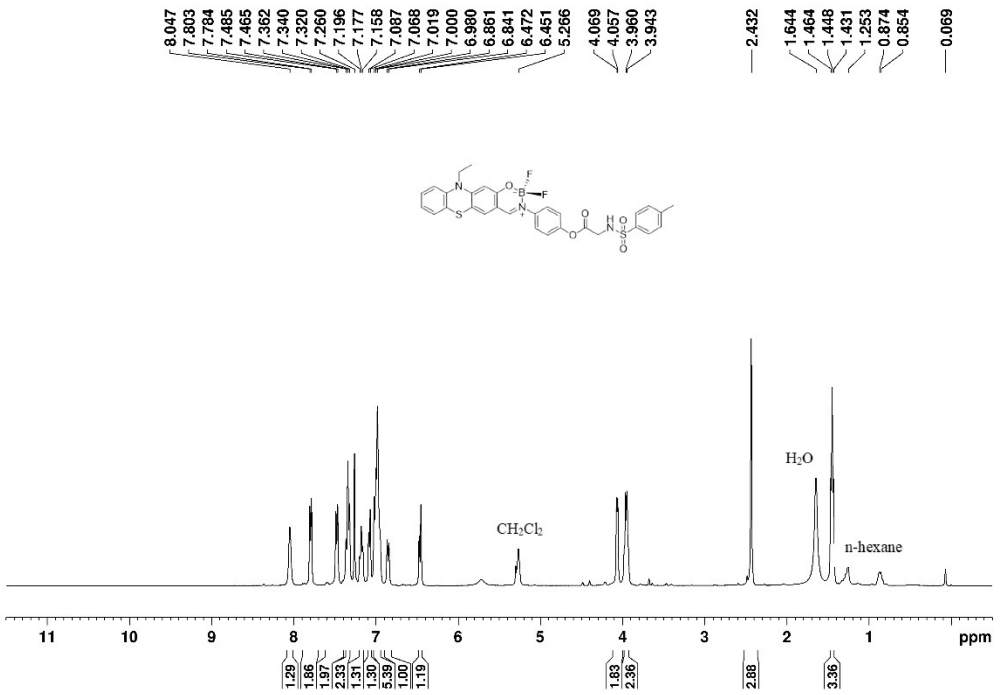

Figure S28. ^{1}H NMR spectrum of **BPTZ5** in $CDCl_3$.

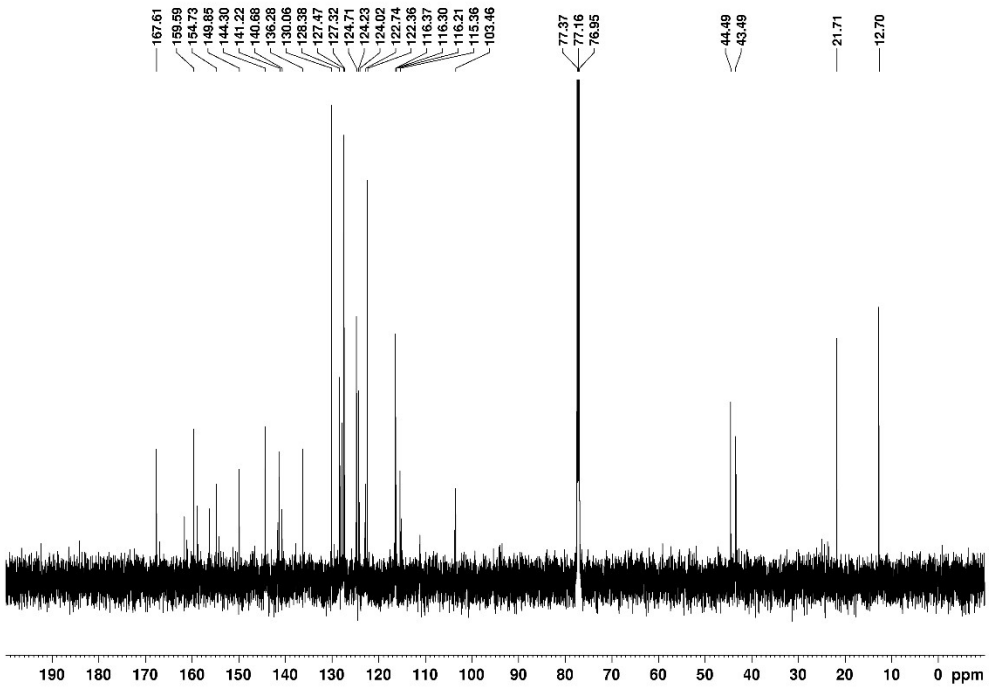

Figure S29. ^{13}C NMR spectrum of **BPTZ5** in $CDCl_3$.

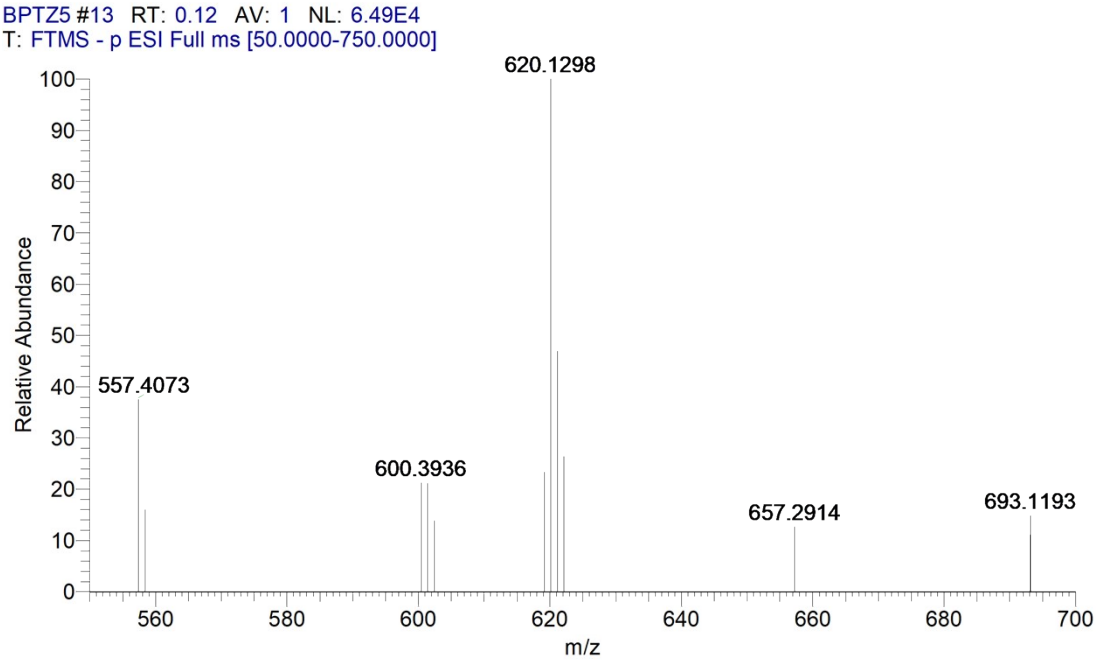

Figure S30. HRMS spectrum of **BPTZ5**.

6. References

1. S. Wang, B. Zhu, B. Wang, P. Fan, Y. Jiu, M. Zhang, L. Jiang and J.-T. Hou, *Dyes and Pigments*, 2020, **173**, 107933-107938.
2. D. A. Frath, S.; Ulrich, G.; Retailleau, P.; Ziessel, R., *Org. Lett.*, 2011, **13**, 3414-3417.
3. Y. Fang, W. Chen, W. Shi, H. Li, M. Xian and H. Ma, *Chem Commun (Camb)*, 2017, **53**, 8759-8762.
4. Q. Sun, J. Xu, C. Ji, M. S. S. Shaibani, Z. Li, K. Lim, C. Zhang, L. Li and Z. Liu, *Anal Chem*, 2020, **92**, 4038-4045.
5. W. Qiao, T. Ma, S. Wang, L. Li, M. Liu, H. Jiang, Y. Wu, J. Zhu and Z. a. Li, *Advanced Functional Materials*, 2021, **31**, 2105452.
6. W. Qiao, P. Yao, Y. Chen, Q. Xiao, L. Zhang and Z. a. Li, *Materials Chemistry Frontiers*, 2020, **4**, 2688-2696.
7. J. T. Hou, B. Wang, Y. Zou, P. Fan, X. Chang, X. Cao, S. Wang and F. Yu, *ACS Sens*, 2020, **5**, 1949-1958.
8. J. Han, S. Yang, B. Wang and X. Song, *Anal Chem*, 2021, **93**, 5194-5200.
9. J.-T. Hou, B. Wang, P. Fan, R. Duan, X. Cao, L. Zhu and S. Wang, *Dyes and Pigments*, 2020, **182**, 108675.
10. B. Deng, M. Ren, X. Kong, K. Zhou and W. Lin, *Sensors and Actuators B: Chemical*, 2018, **255**, 963-969.
11. M. Vedamalai, D. Kedaria, R. Vasita and I. Gupta, *Sensors and Actuators B: Chemical*, 2018, **263**, 137-142.
12. H. Xiao, K. Xin, H. Dou, G. Yin, Y. Quan and R. Wang, *Chem Commun (Camb)*, 2015, **51**, 1442-1445.
13. J. Liu, P. Niu, Y. Rong, W. Chen, X. Liu, L. Wei and X. Song, *Spectrochim Acta A Mol Biomol Spectrosc*, 2021, **261**, 120024.
14. H. Li, Y. Miao, Z. Liu, X. Wu, C. Piao and X. Zhou, *Dyes and Pigments*, 2020, **176**, 108192.
15. X. Bao, X. Cao, Y. Yuan, B. Zhou and C. Huo, *Sensors and Actuators B: Chemical*, 2021, **344**, 130210.
16. H. Cui, P. Hou, Y. Li, J. Sun, H. Zhang, Y. Zheng, Q. Liu and S. Chen, *Journal of Photochemistry and Photobiology A: Chemistry*, 2021, **417**, 113343.
17. P. Wu and H. Xiong, *Talanta*, 2022, **247**, 123584.
18. B. Wang, X. Guo, Z. Liu, Y. Wu and J.-T. Hou, *Chemical Research in Chinese Universities*, 2021, **38**, 609-615.
19. C. Liu, Q. Wang, X. Jiao, H. Yao, S. He, L. Zhao and X. Zeng, *Dyes and Pigments*, 2019, **160**, 989-994.
20. S. Wang, B. Zhu, B. Wang, X. Cao, L. Zhu, J.-T. Hou and L. Zeng, *Chinese Chemical Letters*, 2021, **32**, 1795-1798.
21. V. Natarajan, N. Thirumalaivasan, S. P. Wu and V. Sivan, *Org Biomol Chem*, 2019, **17**, 3538-3544.
22. B. Zhang, X. Yang, R. Zhang, Y. Liu, X. Ren, M. Xian, Y. Ye and Y. Zhao, *Anal Chem*, 2017, **89**, 10384-10390.